

AD-A102 853

MASSACHUSETTS INST OF TECH CAMBRIDGE DEPT OF MATERIALS--ETC F/B 11/9  
MICROSTRUCTURE OF AMORPHOUS AND SEMI-CRYSTALLINE POLYMERS. (U)  
JUN 81 D R UHLMANN.

AFOSR-77-3226

UNCLASSIFIED

AFOSR-TR-81-0629

NL

100-1  
200-1  
400-1

END  
DATE  
ENCL'D  
9-81  
DTIC

DDC FILE COPY

ADA102853

REPORT DOCUMENTATION PAGE		READ INSTRUCTIONS BEFORE COMPLETING FORM	
1. REPORT NUMBER <b>AFOSR-TR-81-0629</b>	2. GOVT ACCESSION NO. <b>AD-A102853</b>	RECIPIENT'S CATALOG NUMBER	
4. TITLE (and Subtitle) <b>MICROSTRUCTURE OF AMORPHOUS AND SEMI-CRYSTALLINE POLYMERS</b>	5. TYPE OF REPORT & PERIOD COVERED <b>FINAL</b>		
7. AUTHOR(s) <b>Donald R. Uhlmann</b>	6. PERFORMING ORG. REPORT NUMBER <b>AFOSR 77-3226</b>		
9. PERFORMING ORGANIZATION NAME AND ADDRESS Massachusetts Institute of Technology Dept of Materials Science & Engineering Cambridge, MA 02139	10. PROGRAM ELEMENT, PROJECT, TASK AREA & WORK UNIT NUMBERS <b>61102F 2303/A3</b>		
11. CONTROLLING OFFICE NAME AND ADDRESS Air Force Office of Scientific Research/NC Bldg. 410, Bolling AFB, DC 20332	12. REPORT DATE <b>7 June 1981</b>		
14. MONITORING AGENCY NAME & ADDRESS (if different from Controlling Office)	13. NUMBER OF PAGES <b>86</b>		
	15. SECURITY CLASS. (of this report) <b>Unclassified</b>		
	15a. DECLASSIFICATION DOWNGRADING SCHEDULE		
16. DISTRIBUTION STATEMENT (of this Report)  Approved for public release; distribution unlimited.			
17. DISTRIBUTION STATEMENT (of the abstract entered in Block 20, if different from Report)  <b>DTIC SELECTED AUG 14 1981</b>			
18. SUPPLEMENTARY NOTES  <b>S A D</b>			
19. KEY WORDS (Continue on reverse side if necessary and identify by block number) Scanning Transmission Electron Microscope Amorphous Thermoplastics Small Angle X-Ray Scattering Random Coil Models Epoxy and Polyimide Resins	Polymers Structures Nodular Hypothesis Microstructures		
ABSTRACT (Continue on reverse side if necessary and identify by block number)  Work carried out under this grant has led to the development of a technique for scanning transmission electron microscope of polymers which seems to offer outstanding promise for the characterization of their structures. When applied to amorphous thermoplastics, the structures are found to be homogeneous down to the limit of resolution to the microscope, with no evidence found for the presence of nodular features or other structures characteristic of regions of local order in the materials. This finding is in accord with the results of small angle neutron scattering studies of same materials. Based on the combined			

DD FORM 1 JAN 73 1473

UNCLASSIFIED

SECURITY CLASSIFICATION OF THIS PAGE (When Data Entered)

results of these studies, it is suggested that the nodular hypothesis be laid to rest and that the structure of flexible chain amorphous polymers be represented by models such as the random coil. The technique of microtoming bulk samples followed by staining with heavy metal atoms and viewing with Z contrast in the scanning transmission electron microscope has also been used with success to characterize the structures of epoxy and polyimide resins. Commercial polyimide films have been shown to be homogeneous on a scale of 50-200 Å, with the scale and form of the heterogeneities varying through the thickness of the film. The structure of epoxy resins presents a more complicated issue. For some resins and some curing conditions, heterogeneous microstructures can be observed. In these cases, the typical scale of the heterogeneities is in the range 100-200 Å. For other epoxy resins and other curing conditions, however, substantially homogeneous microstructures are produced. It seems, therefore, that the production of heterogeneous structures is not a characteristic feature of thermosetting resins. It also seems clear that the structure of the cured resins, as well as their properties and performance characteristics will depend in detail on the resin and conditions of cure. In conclusion, it appears that the technique of high resolution, high contrast electron microscopy--carried out with the scanning transmission electron microscope--is veritably in its infancy. The technique seems to offer particular promise for characterizing the structure of polymers since it permits high contrast images to be obtained with a minimum of electron irradiation and with a permanence to the structural features. It is anticipated that this technique will find many applications during the coming decade.

Accession For	
NTIS GRA&I	<input checked="" type="checkbox"/>
DTIC TAB	<input type="checkbox"/>
Unannounced	<input type="checkbox"/>
Justification _____	
By _____	
Distribution/	
Availability Codes	
Serial and/or	
Special	
A	

UNCLASSIFIED

**AFOSR-TR- 81 - 0629**

15 JUN 1981

**FINAL REPORT**

on

MICROSTRUCTURE OF AMORPHOUS AND SEMI-CRYSTALLINE POLYMERS

**3226**  
(AFOSR 77- )

Submitted to

AIR FORCE OFFICE OF SCIENTIFIC RESEARCH

Professor D. R. Uhlmann

Massachusetts Institute of Technology

7 June 1981

Approved for public release  
Distribution unlimited.

## I. INTRODUCTION

This report summarizes the results of investigations carried out under AFOSR grant 77-3226 during the period February, 1977 to October, 1980. The work has already resulted in six technical publications, copies of which are appended to the present report.

The discussion on the following pages is intended as a supplement to the results described in the papers, and will direct particular attention to highlights of the work and to aspects of the work which are not discussed in the papers.

The work was carried out under the supervision of Professors D. R. Uhlmann and J. B. Vander Sande. The students who have carried out work under the grant include: Miss M. Meyer, who was awarded an M.S. degree from MIT for work carried out in the area; and Messrs. G. Di Filippo and B. Jang, both of whom expect to receive their Sc.D. degrees during the coming year. The activity has been a most stimulating one for both students and faculty; and the principal investigators wish to acknowledge their gratitude for the support of AFOSR which made it possible.

8 1 8 14 0 25

AIR FORCE OFFICE OF SCIENTIFIC RESEARCH (AFSC)  
NOTICE OF TRANSMITTAL TO DTIC  
This technical report has been reviewed and is  
Approved for public release IAW AFR 130-12.  
Distribution is unlimited.  
MATTHEW J. WILMER  
Chief, Technical Information Division

AIR FORCE OFFICE OF SCIENTIFIC RESEARCH  
NOTICE OF TRANSMITTAL TO DTIC  
This technical report has been reviewed and is  
Approved for public release IAW AFR 130-12.  
Distribution is limited.  
MATTHEW J. WILMER  
Chief, Technical Information Division

## II. RESULTS OF INVESTIGATIONS, STRUCTURE OF AMORPHOUS THERMOPLASTICS

The most widely accepted model for the microstructure of most unoriented amorphous polymers is that of a random coil. This model has been widely used to represent the properties of polymers, including their elasticity and flow behavior. Beginning about ten years ago, however, a number of investigations--based primarily on electron microscope observations--cast doubt on the random coil model. The essential and surprising feature of these results, which are summarized in Ref. 1, was the observation of heterogeneities (present in large volume fractions) in nearly all amorphous polymers examined. These heterogeneities, termed nodules, were observed on a scale of 30-200 Å. Their observation was taken as strong evidence against the random coil model and strong support for the existence of local order in the materials. The degree of order was suggested as intermediate between that of a random coil and that expected for a crystalline structure.

A forceful defense of the random coil model and a recapitulation of its utility for describing the properties of amorphous polymers was presented by Flory (2). As he noted, the observation of heterogeneities in glassy polymers stands in contrast with the success of the random coil model in representing many of the properties of these materials. Further, the occurrence of nodular structures is difficult to reconcile with the results of studies of small angle neutron scattering (3, 4, e.g.) and small angle X-ray scattering (5, 6, e.g.) from several of the same polymers.

Small angle neutron scattering indicates radii of gyration for the bulk polymers which agree within experimental error with the dimensions of the chains in theta solvents (which are widely agreed to be those of a random coil). The small angle X-ray scattering (SAXS) studies, carried out by the principal investigator and by Professor Fischer in Germany, are inconsistent in both the magnitude and angular dependence of the SAXS intensity with the presence of nodular structures as representative of the bulk material.

In work supported by the AFOSR grant, transmission electron microscopy was carried out on amorphous polycarbonate, polystyrene, polyethylene terephthalate and polyvinyl chloride. Appropriately thin samples of these polymers were cast from solutions using the same techniques as those employed in studies where nodular structures were reported.

For all four polymers, the structures were featureless down to the limit of resolution of the electron microscope. No evidence was found in either bright field or dark field for nodular features. Series of through-focus electron micrographs showed the absence of observable structure in the in-focus micrographs, and indicated that apparent structure could be developed in the micrographs by going to under-focus or over-focus conditions (7).

These results suggested that the fine-scale (less than 30 Å) apparent structure seen in some previous investigations could reflect the use of electron microscopes of insufficient resolution or the lack of proper focus in taking the micrographs. To explain the observations of larger nodules, other rationales seem required (e.g., the nodules may represent

surface rather than bulk features of the polymers) .

The combined weight of these studies led to the conclusion that the structure of amorphous thermoplastics should be represented by random array models such as the random coil. At the 1979 Faraday Discussion, it was suggested by the principal investigator (8) and by Flory (9) that the controversy concerning local order in amorphous thermoplastic polymers could be laid to rest and that attention should now be directed to more fruitful areas.

### III. SCANNING TRANSMISSION ELECTRON MICROSCOPE OF POLYMERS

The observations on amorphous polymers described in previous sections were carried out using a Vacuum Generators HB-5 Scanning Transmission Electron Microscope. Considerable attention was directed during the period of the grant to developing techniques for using this instrument to elucidate the structural features of polymeric materials. The capabilities of the STEM in this regard will be discussed in the present section.

Several types of STEM are currently in use; they can be divided into roughly three categories based on origin and philosophy of design. First are the "dedicated" STEM's, pioneered by Crewe and his coworkers (10), which use a field-emission electron gun housed in the ultra-high vacuum system. A conventional TEM may also be equipped with a scanning attachment and an electron detector and/or spectrometer, yielding what may be referred to as a TEM(S). Finally, in practice an SEM may be fitted with a transmission stage; in this case the designation SEM(T) may be most appropriate.

In all three cases, the basic mode of operation is identical. An extremely fine probe of electrons, ideally 2 to 3 Å in diameter, is scanned across the specimen, which is in the form of a thin foil. Various products of the electron-specimen interaction are then collected and used for image formation or microanalysis (see Fig. 1). The electrons which have passed through the sample and have either been forward-scattered with no change in energy or direction, inelastically scattered, or elastically scattered can be collected by some type of electron

detector and used to modulate the intensity of a cathode-ray tube, forming an image of the internal structure of the material.

Fig. 2 is a schematic ray diagram of the electron-optical column of a dedicated STEM, the Vacuum Generators (V.G.) HB-5. The electron source is a cold cathode field-emission gun located at the base of the column. The gun is housed in an ultra-high-vacuum system, with pressure  $\leq 2 \times 10^{-11}$  torr, necessary for reliable, noise-free operation and long lifetime of a cold-cathode field-emission tip.

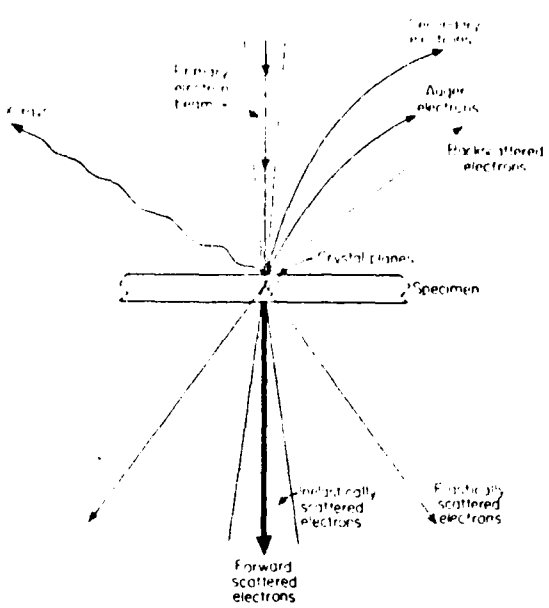


**Fig. 1.** Possible products of interaction of electron beam with crystalline sample.

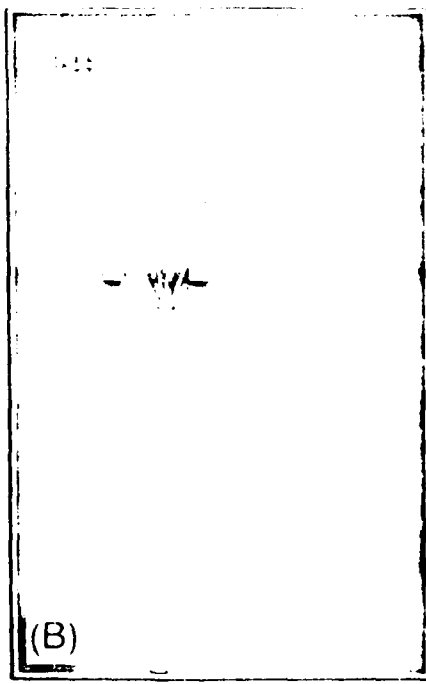


**Fig. 2.** Ray diagram showing important column elements and electron ray path for V.G. STEM in normal imaging mode. Note position of annular detector.

The electron beam thus produced is then accelerated to a maximum of 100 kV potential. Two electromagnetic lenses demagnify the electron source to a final probe diameter as small as  $3 \text{ \AA}$  at the specimen, and a set of double deflection electromagnetic coils scan this probe orthogonally across the specimen. An annular detector is situated to collect the electrons scattered through angles  $0.02 \text{ rad} \leq \theta \leq 0.2 \text{ rad}$ , while the forward-scattered and inelastically scattered electrons pass through the center of this detector. These electrons are collected by the electron spectrometer-bright-field detector assembly at the top of the instrument. The spectrometer allows electrons of a selected energy to pass into the bright-field detector, which produces an image comparable to the bright-field image in a TEM (when "unsacattered" zero-loss electrons are detected). The annular detector in the STEM collects the bulk of the elastically scattered electrons. Since the annular detector is nearly 100% efficient in collecting elastically scattered electrons, compared with conventional TEM, dark-field images can be obtained with a minimum electron dose, especially when the beam scanning is carefully controlled. In addition, for the annular detector the contrast mechanisms which are most important in polymeric materials are maximized, i.e., thickness contrast and atomic-number contrast.

### A. The Theory of High Contrast Imaging

Consider a thin polymer film where one phase, or one class of microstructural feature, has been lightly stained with a heavy element such as U or Os. If a total of  $N$  electrons is incident on the specimen, then  $N_e$  electrons will be elastically scattered,  $N_{in}$  will be inelastically scattered, and  $N_o$  ( $= N - N_e - N_{in}$ ) will be unaffected by the sample. Theoretical scattering cross-section calculations have been made by Lenz (33) and these calculations can be simplified to yield

$$\frac{N_e}{N} = \frac{46.5Z^{4/3}}{\sigma_b \cdot V} n = \frac{n\sigma_e}{\sigma_b} \quad (1)$$

$$\frac{N_{in}}{N} = \frac{868.Z^{1/3}}{\sigma_b \cdot V} n = \frac{n\sigma_{in}}{\sigma_b} \quad (2)$$

for a thin sample where  $Z$  is the atomic number,  $V$  is the accelerating voltage,  $\sigma_b$  is the cross-sectional area of the electron beam, and  $n$  is the number of atoms in the beam. Also,  $\sigma_e$  and  $\sigma_{in}$  are the elastic and inelastic scattering cross-sections with the units of  $\text{Å}^2$ .

Elastic scattering occurs at large scattering angles (50 to 100mr) compared to the convergence angle of the illumination (20 mr), so that most elastically scattered electrons are scattered outside the cone of illumination. The inelastic scattering process, on the other hand, is such that the angles of scattering are small (1 mr), and most inelastically scattered electrons stay within the illumination cone (see Fig. 1). Since the annular detector (see Fig. 2) subtends several hundred milliradians while the hole in the detector allows

electrons which subtend 20 mr or less to pass through, this detector measures predominantly  $N_e$ .

The electrons that pass through the hole in the detector can be separated into the two components  $N_o$  and  $N_{in}$  by means of the electron spectrometer. Clearly, from Equations (1) and (2),  $N_e/N_{in} \approx Z/19$  and this relation is independent of specimen thickness or the energy of the electron beam to a first approximation.

Before attempting to quantitatively assess the application of these techniques to polymer microstructures, it may be wise to "step back" and qualitatively describe a scenario for image enhancement. Consider a simplified polymer sample consisting of carbon (C) atoms only, where a "second phase" exists which can be lightly "stained" with a few uranium (U) atoms. Now consider two columns in a thin section of the polymer, one column contains only C atoms, the other column contains only the "second phase" with associated U atoms. In a divided image (taking the elastic image and dividing it by the inelastic image,  $N_e/N_{in}$ ), the contrast ( $\equiv \Delta I/I$ , where I is intensity) for these two columns will be proportional to

$$\frac{Z_U/19 - Z_C/19}{Z_C/19} = \frac{\frac{92}{19} - \frac{6}{19}}{\frac{6}{19}} = 14.33$$

a very large contrast number.

A slightly more sophisticated approach might assume that in the second phase one out of every 100 atoms is U, i.e.,  $n_C/n_U = .01$ . Then for the second phase

12.

$$\frac{N_e^{C+U}}{N} = \frac{n_u \sigma_e^U + n_c \sigma_e^C}{\sigma_b} \quad (3)$$

and for the matrix

$$\frac{N_e^C}{N} = \frac{n_c \sigma_e^C}{\sigma_b} \quad (4)$$

and, for the second phase

$$\frac{N_{in}^{C+U}}{N} = \frac{n_u \sigma_{in}^U + n_c \sigma_{in}^C}{\sigma_b} \quad (5)$$

for the matrix

$$\frac{N_{in}^C}{N} = \frac{n_c \sigma_{in}^C}{\sigma_b} \quad (6)$$

where  $n_C$  = the number of carbon atoms in the beam

$n_U$  = the number of uranium atoms in the beam and the other parameters have been previously described.

Now, for a divided image, the second phase is

$$\frac{N_e^{C+U}}{N_{in}^{C+U}} = \frac{n_u \sigma_e^U + n_c \sigma_e^C}{n_u \sigma_{in}^U + n_c \sigma_{in}^C} \quad (7)$$

for the matrix

$$\frac{N_e^C}{N_{in}^C} = \frac{\sigma_e^C}{\sigma_{in}^C} \quad (8)$$

Using the definition of contrast

$$\frac{\Delta I}{I} = \frac{\frac{N_e^{C+U}}{N_{in}^{C+U}} - \frac{N_e^C}{N_{in}^C}}{\frac{N_e^C}{N_{in}^C}} = \frac{\frac{N_e^{C+U}}{N_{in}^{C+U}}}{\frac{N_e^C}{N_{in}^C}} - 1$$

$$\frac{N_e^C}{N_{in}^C}$$

$$\frac{N_e^C}{N_{in}^C}$$

$$(9)$$

Therefore

$$\frac{\Delta I}{I} = \frac{\frac{n_u \sigma_e^U + n_c \sigma_e^C}{n_u \sigma_e^U + n_c \sigma_e^C}}{\frac{n_u \sigma_e^U + n_c \sigma_e^C}{n_u \sigma_e^U + n_c \sigma_e^C}} \cdot \frac{\frac{\sigma_{in}^C}{\sigma_e^C}}{\frac{\sigma_{in}^C}{\sigma_e^C}} - 1$$

$$(10)$$

and substituting  $n_u = .01 n_c$

$$\frac{\Delta I}{I} = 0.35 = 35\%$$

far in excess of the 5% considered necessary for visibility. Thus, divided images of the type described above for very lightly stained polymers will yield contrasty images capable of elucidating the polymer microstructure.

#### B. Radiation Damage in Polymers

The ability to characterize the state of inhomogeneity of such epoxies represents a major step forward in the application of electron microscopy to the microstructural analysis of polymers. It has opened opportunities for characterizing the microstructures of polymers as functions of process history, including cure conditions, stress applied to the samples, and the general thermomechanical history of the specimens. Certainly, the presence of such heterogeneities in partially-

cured epoxies has important implications for the use of these materials in high performance application. Also important, however, is the potential for "seeing things" in polymers that could not be seen with any other technique.

In the present work, a combined technique has been developed for studying polymers. This technique includes ultra microtomy of the polymers, followed by staining of the resulting thin sections with heavy metal ions and viewing with Z enhancement in the STEM. The combination of staining thin sections with heavy metal salts and viewing with Z enhancement in the scanning transmission electron microscope seems to provide the capability of characterizing with confidence the structural features of polymeric materials. As used in the present studies, with staining by heavy metal ions, it has been possible to elucidate the structure of a broad range of resins with a clarity that is not possible using transmission electron microscopy of unstained samples and with a confidence that is usually not possible using replication electron microscopy.

Since the technique employs microtomed sections, it offers the possibility of characterizing the structure of bulk polymers. Based on experience in our laboratory, the process of ultramicrotomy requires considerable care to avoid introducing artifacts (chatter marks, crazing, etc.) in the thin sections; but once mastered, the technique

can be used routinely and efficiently. Use of the heavy metal stain not only provides increased contrast for viewing structural features, it also provides increased permanence to the features on viewing in the electron microscope. That is, while short-range molecular rearrangements induced by the electron irradiation can wipe out structural features such as crystals at modest radiation doses, relatively long-range diffusion of the stain is required to wipe out the perception of the structural features in stained polymers; and this requires substantially higher radiation doses.

#### IV. STRUCTURE OF POLYIMIDE AND EPOXY RESINS

In work carried out under the present grant, the feasibility of using heavy metal atoms as stains and combining the corresponding bright field and annular dark field images of a specimen to provide greatly enhanced contrast has been explored. Uranyl acetate has now been used successfully as a staining agent for a number of thermosetting polymers, including epoxies and polyimides. Although the selectivity of staining of the different regions is small, suitable contrast can be developed by the Z contrast technique described above, which involves combining the bright field and annular dark field images of the sample.

Results obtained in this way are shown in Fig. 3 for an Epon 812 epoxy resin cured with NMA, DDSA and BDMA at 70°C for 2 hours. Without the use of uranyl acetate as a staining agent, the microstructure appears homogeneous. That is, the differences in density between the regions of the specimen and the lack of structural order produce insufficient contrast for structural features to be discerned in the electron microscope. With uranyl acetate staining but without the heightened image contrast provided by the Z contrast technique of the STEM, structural inhomogeneities are perceived; but their characteristics cannot be resolved with confidence. Using uranyl acetate as a staining agent, and combining the bright field and annular dark field images, the inhomogeneous microstructure of this cured epoxy is apparent.

Difficulties associated with electron irradiation damage in polymers have reduced the effectiveness of electron microscopy in many polymer research areas. The M.I.T. STEM has been designed to

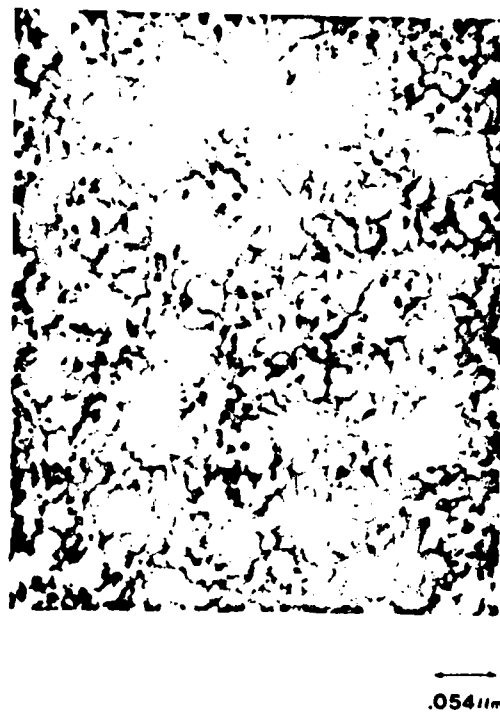


Fig. 3 Microstructure of Epon 812 epoxy resin cured with NMA,  
DSA and BDMA at 70°C for two hours.

optimize its capabilities for accomplishing low dosage electron microscopy while maintaining excellent resolution. This has been done by equipping the microscope with a scan converter (image storage device) that allows images to be stored after which the beam is diverted from the sample, thereby eliminating additional radiation damage. The operator of the instrument can then interact with the scan converter to choose a small area in the stored image to be used for magnification change, focusing, aberration correction, etc. This area is then scanned by the beam to accomplish these corrections. An unirradiated area is then chosen (this area existed on the original stored image) and that area is photographed with a scan of the area. In short, a high quality image of an area can be obtained with only two scans of that area. The first scan, done at low magnification and therefore low electron dosage, produces the stored image. The second scan, of a selected area, provides the final, hard copy. Two scans are considered to be the lower limit in dosage to produce a hard copy of a quality image.

The scale of the inhomogeneities seen in Figure 3 is similar to that inferred from small angle X-ray scattering (SAXS) studies of the same epoxy resin cured under the same conditions. This SAXS work is described in detail in the appended paper from the Journal of Polymer Science. As indicated there, the small angle X-ray scattering (SAXS) from an Epon 812 and two Epon 828 (one amine-cured and one anhydride-cured) epoxy resins has been measured using a Bonse-Hart system. The data cover the angular range ( $2\theta$ ) between 20 sec and 60 min. After correction for absorption, background and vertical beam

divergence, they have been placed on an absolute basis by comparison with the scattering from a previously studied polycarbonate sample. The corrected absolute intensity decreases strongly with increasing angle between 20 sec and 2 min, decreases more gradually between 2 and 20-30 min, and reaches a nearly constant asymptotic value at larger angles. The magnitude of the intensity in the constant-intensity region is close to the value predicted by thermodynamic fluctuation theory for fluids applied at the glass transition temperature. The increase in intensity at angles smaller than 20-30 min is associated with heterogeneities in the cured resins. These heterogeneities cover a range of sizes in all samples, from less than 100 Å to more than 1000 Å, with the most frequently occurring size in the range 100-200 Å.

As further examples of the combined techniques of microtoming, staining, and viewing with Z contrast in the STEM, a series of investigations were carried out on polyimide films. Particular attention was directed to commercial polyimide films such as du Pont's H film. In all cases, the film was microtomed, stained with uranyl acetate, and examined using the Z contrast STEM technique. In all cases, the structure was seen to be markedly heterogeneous on a scale of 50-200 Å. The scale and detailed form of the structure was observed to vary continuously through the thickness of the film--very likely reflecting the solvent casting procedure used in its manufacture. The presence of such heterogeneities has important

implications for the performance of these materials, particularly in applications which depend on the permeability of a substance such as water through the films.

V. CONCLUDING REMARKS

As indicated in the preceding sections, work carried out under the present grant has led to the development of a technique for scanning transmission electron microscope of polymers which seems to offer outstanding promise for the characterization of their structures. When applied to amorphous thermoplastics, the structures are found to be homogeneous down to the limit of resolution to the microscope, with no evidence found for the presence of nodular features or other structures characteristic of regions of local order in the materials. This finding is in accord with the results of small angle X-ray scattering, wide angle X-ray scattering and small angle neutron scattering studies of the same materials. Based on the combined results of these studies, it is suggested that the nodular hypothesis be laid to rest and that the structure of flexible chain amorphous polymers be represented by models such as the random coil.

The technique of microtomining bulk samples followed by staining with heavy metal atoms and viewing with Z contrast in the scanning transmission electron microscope has also been used with success to characterize the structures of epoxy and polyimide resins. Commercial polyimide films have been shown to be homogeneous on a scale of 50-200 Å, with the scale and form of the heterogeneities varying through the thickness of the film. The structure of epoxy resins presents a more complicated issue. For some resins and some curing conditions, heterogeneous microstructures can be observed. In these cases, the typical scale of the heterogeneities is in the range 100-200 Å.

For other epoxy resins and other curing conditions, however, substantially homogeneous microstructures are produced. It seems, therefore, that the production of heterogeneous structures is not a characteristic feature of thermosetting resins. It also seems clear that the structure of the cured resins, as well as their properties and performance characteristics will depend in detail on the resin and conditions of cure.

In conclusion, it appears that the technique of high resolution, high contrast electron microscopy--carried out with the scanning transmission electron microscope--is veritably in its infancy. The technique seems to offer particular promise for characterizing the structure of polymers since it permits high contrast images to be obtained with a minimum of electron irradiation and with a permanence to the structural features. It is anticipated that this technique will find many applications during the coming decade.

REFERENCES

1. G.S.Y. Yeh: Crit. Rev. Macromol. Chem. 1, 173 (1972).
2. P.J. Flory: Macromol. Chem. 8, 1 (1973).
3. D.G.H. Ballard, G.D. Wignall and J. Schelten: Europ. Polymer J. 9, 965 (1973).
4. G.D. Wignall, D.G.H. Ballard and J. Schelten: Europ. Polymer J. 10, 861 (1974).
5. A.L. Renninger, G.G. Wicks and D.R. Uhlmann: J. Polymer Sci., Phys. 13, 1247 (1975).
6. J.H. Wendorff and E.W. Fischer: Kolloid-Z. u. Z. Polymere 251, 876 (1973).
7. M. Meyer, J.B. Vander Sande and D.R. Uhlmann: J. Polymer Sci., Phys. 16, 2005 (1978).
8. D.R. Uhlmann: "Electron Microscopy and SAXS Studies of Amorphous Polymers", Faraday Discussions of the Royal Society of Chemistry 68, 22 (1979).
9. P.J. Flory: "Structure of Amorphous Polymers", Faraday Discussions of the Royal Society of Chemistry 68, 38 (1979).
10. A.V. Crewe, J. Wall, and L.M. Welter, J. Appl. Phys. 39, 5861 (1968).

PHYSIKALISCHE GESELLSCHAFT DER DEUTSCHEN DEMOKRATISCHEN REPUBLIK  
Sektion Physik der Wilhelm-Pieck-Universität Rostock

**Kurzfassungen  
der Vorträge**

2. Tagung Festkörperphysik  
**AMORPHE FESTKÖRPER**  
26.-28. November 1980  
in Rostock

## THE ATOMIC STRUCTURE OF GLASSES

Hilmaun, D. R.

Department of Materials Science and Engineering

Massachusetts Institute of Technology, Cambridge, Mass., USA

Information on the structure of glasses on various scales is reviewed. Particular attention is directed to models used to represent the structure of glass, and to the results of various determinations of glass structure. Attention is directed to both oxide and polymer glasses. It is suggested that random array models seem to provide the best description of structure for most glasses, but that the arrays may consist of units larger than the basic structural units of the materials.

#### I. INTRODUCTION

Early controversies between proponents of the crystallite and random network models of oxide glass structure were generally decided in favor of the random network model, based largely on the arguments advanced by Warren (1, e.g.) considering both the breadths of the wide angle diffraction maxima and the absence of very pronounced X-ray scattering at small angles.

Because of the wide acceptance of the random network model, it came as a great surprise to many when electron microscope studies of a number of glasses indicated the presence of heterogeneities on a scale of 50-200 Å. The heterogeneities were present in large volume fractions (in the range of 50%), and were seen in both single component and multi-component glasses, using both replication and direct transmission electron microscopy.

The phenomenology of phase separation in oxide glasses has been reviewed by a number of authors (2, 3, e.g.). Microstructures consisting of discrete second-phase particles are generally seen near the boundaries of miscibility gaps (volume fractions of second-phase material less than 15-20%), while interconnected microstructures are often, but not invariably, observed in the central regions of miscibility gaps.

In many glass-forming systems, even more complex phase arrays can be produced as a result of liquid-liquid immiscibility. It has been demonstrated, for example, that a multiplicity of amorphous phases can be produced by appropriate heat treatment of various compositions (4, e.g.), and that secondary phase separation is a phenomenon of potential importance in many glasses (5, 6, e.g.).

Caution should be exercised in inferring the mechanism of phase separation from the form of the observed structures. It has been noted, for example, that interconnected microstructures can be produced by the formation, growth

and coexistence of discrete second-phase particles (7, e.g.) and that discrete particle structures can be produced by heat treatment of interconnected structures (7, 8, e.g.). It has also been noted that inclusion of the leading higher-order nonlinear terms in the theory of spinodal decomposition leads to a breaking of the interconnectivity seen in the early stage, linear treatment.

### II. CRYSTALLINE

In an already-classic paper, Mozzi and Warren (9) used the technique of fluorescence excitation to eliminate Compton scattering, and obtained reliable data out to large values of  $\sin\theta/2$ . They found the random network model to provide the best representation of the structure of glassy  $\text{SiO}_2$ ; and they determined that the essential structural randomness of the glass resulted both from a variation in Si-O-Si bond angles, which is notably broader than that of crystalline polymorphs of  $\text{SiO}_2$ , as well as from a distribution of rotation angles of one tetrahedron with respect to an adjacent tetrahedron.

Mozzi and Warren originally suggested a mean Si-O-Si angle of about  $144^\circ$ . Re-analysis of their data by Silva et al. (10) considered different damping factors and suggested a mean Si-O-Si angle of  $151.5\text{--}152.2^\circ$ . Subsequent work by Uhlmann and Weeks (11), who also considered different values of the damping factor, suggested a mean Si-O-Si angle of  $147^\circ$ . This value was based on a damping factor of 0. The distribution of rotation angles of one tetrahedron with respect to another was found to be random. That is, no evidence was found for the edge-opposite-face orientations of tetrahedra which are commonly seen in crystalline silicates.

In the case of  $\text{CaO}_2$ , it has been found (11, 12) that the distribution of O-Si-O angles in the glass is nearly as sharp as that in the crystal. It was suggested that the essential structural randomness of glassy  $\text{CaO}_2$  results from a random distribution of rotation angles of one tetrahedron with respect to an adjacent tetrahedron.

Weeks and Uhlmann (11, 13) also found that the random network model provided the best representation of the structure of a number of third-phase alkali silicate glasses. Some evidence was found, however, for the pairing of alkali ions in the structure. Evidence for pairing has been provided by other diffraction studies of multicomponent glasses, as discussed in the excellent review of this and other aspects of the structure of oxide glasses by Pethrick (14).

Other workers have interpreted diffraction data on these glasses using modified crystallite models (15, e.g.). Support for the random network model

has, however, been provided by a series of small angle X-ray scattering studies (16-19, e.g.). For both  $\text{SiO}_2$  and  $\text{GeO}_2$ , an asymptotic small angle intensity is observed, whose magnitude is within a factor of 1.5 of that predicted from thermodynamic fluctuation theory for thermal density fluctuations frozen-in at the glass transition. These findings provide strong evidence against the occurrence of crystallites or other heterogeneous features in the basic structural units of the materials.

A significant question has arisen concerning whether the thermal density fluctuations are in fact frozen-in at the glass transition, or whether one should anticipate a change in the fluctuation scattering with decreasing temperature below the glass transition. For a number of glassy polymers, Wendorff and Fischer (20) found in an important study that the asymptotic scattering decreased linearly with falling temperature below the glass transition.

In contrast to this work is the most impressive study of Poral-Koshita and his colleagues (18) who measured the asymptotic small angle X-ray scattering from glassy  $\text{SiO}_2$  over a range from room temperature to 1100°C. It was found that the level of asymptotic scattering was constant over this broad range of temperature, indicating strongly that the thermal density fluctuations are frozen-in at the glass transition.

The origin of the difference between polymer glasses and oxide glasses in this regard remains unexplained. Wendorff and Fischer suggest that the density fluctuations below the glass transition are proportional to the compressibility of the sample at  $T_g$  and to the actual temperature of the sample. The rationale for the change in density fluctuations below the glass transition is far from convincing; and it should be noted that the data of Poral-Koshita and his colleagues cover a much broader range of temperature, even when scaled by the glass transition temperature, than do the data on the polymer glasses. Considering the importance of density fluctuations to matters of present technological interest, this area seems to merit closer attention.

Although the wide angle and small angle X-ray diffraction studies of  $\text{SiO}_2$  and  $\text{GeO}_2$  glasses seem best represented by random network structures, electron microscope observations (21, e.g.) suggested the presence of domains (termed micelles) having a degree of order intermediate between that of a random array and a perfect crystal. The electron microscope evidence was re-examined by Seward and Uhlmann (22) in the case of  $\text{SiO}_2$ . It was found that heterogeneities were only sometimes seen, and when seen, depended on the techniques used to prepare samples for the electron microscope observations. It was

suggested, therefore, that the original observations of heterogeneity in single-phase glasses should not be taken as representative of the structure of the materials.

In the case of  $B_2O_3$ , the structure does not seem to be composed of a random network of  $BO_3$  triangles. Rather, a random array of boroxyil units (23) or an array of twisting ribbons of triangles without long-range correlations (24) have been suggested to represent the structure.

The results obtained on  $B_2O_3$  and the models suggested to represent the structure raise an interesting issue with respect to the random network model. Specifically, in the case of  $B_2O_3$ , the random arrays which provide the best description of experimental data are composed of units which are larger than the basic structural units of the material ( $BO_3$  triangles). This result may be applicable as well to other glasses, where the random network may consist of entities larger in scale than the fundamental units of the structure.

With this qualification, it should be noted that for all of the single-phase oxide glasses studied using modern diffraction and computational techniques, the best representations of the structure are not provided by models based on crystallites, micelles or nodules, paracrystals, or structures having fivesfold symmetries. Rather, the best descriptions of the structure seem to be provided by random array models.

The term random array has been used as a generalization of the random network model, since modification of the model is obviously required for regions of composition where the formation of three-dimensional networks is not possible—e.g., regions of the metasilicate compositions in alkali-silicate systems where even the crystals are composed of chains of  $SiO_4$  tetrahedra, or the existing new classes of oxide glasses produced by rapid quench techniques in which network formation is most unlikely. For such materials, as well as for linear polymers, the generalized picture is that of a random array in which the structural elements are randomly arranged and in which no unit of the structure is repeated at regular intervals in three dimensions.

In light of the success of the random network model in representing the structure of many oxide glasses, it would also seem desirable to examine in detail the principles upon which such a model is based. As noted previously (25), the original conceptual basis of Zachariasen (26), that "the substance can form extended three-dimensional networks lacking periodicity with an energy content similar to that of the corresponding crystal network", seems highly simplified. A number of classic oxide glass formers have, in fact, rather large differences

in energy between liquid and crystal (e.g.,  $F_0^0$  and  $K_{\text{J}}^0$  and  $K_{\text{J}}^{\text{cr}}$ ). Further, while a small difference in energy between liquid and crystal would imply a relatively small driving force for crystallization at a given undercooling, and hence a relatively small crystal growth rate, it would also imply a relatively small crystal-liquid surface free energy, and hence a relatively high nucleation rate (even allowing for the effect on driving force).

To the present author's knowledge, there have been no studies which have unequivocally elucidated the structure of the individual phases in two-phase or multi-phase glasses. In light of the success of the random array models in representing the structure of both single component and single phase binary glasses, it seems reasonable to adopt the working hypothesis that the structures of the individual phases in phase-separated glasses can also be described by such models. Before closing, it should be noted that a great deal of the interest and activity in the field of glass science is concerned with glasses which are unfamiliar to many traditional glass technologists. Examples of these glasses are tungstate and nitrate glasses, metal alloy glasses and polymer glasses. In each of these areas, important insights can be provided by the traditional glass scientists; and we in the oxide glass community should be encouraged to broaden our scope and participate in the activity. As an example of work in other fields where structural questions have been addressed with vigor, consider the case of polyac glass, whose structure was traditionally represented by the random cell model (27), which can be regarded as a form of the random array model. This model received very wide acceptance in the field of polymers, and was considered to provide a useful description of both structure and properties.

In developments closely parallel to those in the field of oxide glasses discussed above, but occurring later in time, electron microscope observations (28, e.g.) of a large number of glassy thermoplastics indicated the presence of heterogeneities on a scale of 30-200 Å. These heterogeneities, termed nodules, were reported to be present in large volume fractions (in the range of 50%), were seen in both stereoregular and atactic polymers, and were observed in both bright field and dark field electron microscope. These nodular heterogeneities were taken as strong evidence against the random cell model, and strong support for the existence of regions of local order in the materials. Also similar to developments in the field of oxide glasses, subsequent investigations of the structure of amorphous thermoplastics have indicated that the nodular features are not representative of the structure of the bulk polymers. This conclusion is based on direct structural investigations of four types: (1) small angle neutron scattering (29, e.g.); (2) wide angle X-ray

scattering (30, e.g.); (3) small angle X-ray scattering (31, e.g.); (4) light scattering (32, e.g.). In addition, investigations of the optical anisotropies of polymers have provided further evidence against the existence of ordered regions as characteristic structural features of glassy polymers.

In conclusion, the field of glass structural studies is a dynamic and highly interesting area for scientific investigations. Considerable progress has been made in elucidating the structure of the traditional network-based oxide glasses, and the prospects are quite good for further advances in the field. The focus of glass structural studies seems, however, to have shifted to novel oxide glasses and to a broad range of non-oxide glasses. The momentum in this direction seems, if anything, likely to increase in the coming decade.

#### ACKNOWLEDGEMENTS

Financial support for the present work was provided by the National Science Foundation and by the Air Force Office of Scientific Research. This support is gratefully acknowledged, as are stimulating discussions with Professors B.E. Warren of MIT and E.A. Poral-Koshits of Leningrad.

AFOSR-77-3226

#### REFERENCES

1. B.E. Warren and J. Blcoet: *J. Am. Ceram. Soc.*, **21** (1938) 49.
2. D.R. Uhlmann and A.G. Folbeck: *Phys. Chem. Glasses* **17** (1976) 146.
3. W. Vogel: *J. Non-Cryst. Solids* **25** (1977) 170.
4. W. Vogel: *Structure and Crystallization of Glasses* (Pergamon, 1971).
5. T.P. Seward, D.R. Uhlmann and D. Turnbull: *J. Am. Ceram. Soc.* **51** (1968) 278.
6. E.A. Poral-Koshits, and V.T. Averlovo: *J. Non-cryst. Solids* **1** (1966) 29.
7. T.P. Seward, D.R. Uhlmann & D. Turnbull: *J. Am. Ceram. Soc.* **51** (1968) 634.
8. W. Haller, D.H. Blackburn & J.H. Stoenes: *J. Am. Ceram. Soc.* **57** (1974) 120.
9. R.L. Mozzi & B.E. Warren: *J. Appl. Cryst.* **2** (1969) 164.
10. J.R.G. Silva, D.G. Pinatti, S.T. Anderson & M.L. Pidgeon: *Phil. Mag.* **31** (75) 213.
11. D.R. Uhlmann & G.G. Wicks: In *Wiss. Ztschr. Friedrich Schiller Univ. Jena*, **79**.
12. A.J. Leibbether & A.C. Wright: *J. Non-cryst. Solids* **2** (1972) 37.
13. G.G. Wicks: Sc.D. Thesis, MIT, 1975; to be published.
14. E.A. Poral-Koshits: *J. Non-cryst. Solids* **25** (1977).
15. J.H. Kunert & J. Karle: *Acta Cryst.* **29A** (1973) 762.
16. D.L. Weinberg: *J. Appl. Phys.* **33** (1962) 1012.
17. A. Pierre, D.R. Uhlmann & F.H. Molea: *J. Appl. Cryst.* **5** (1972) 216.
18. E.A. Poral-Koshits, V.V. Galubkov & A.P. Titov: In *Proc. X Int'l. Congress on Glass*.
19. A.L. Renninger & D.R. Uhlmann: *J. Non-cryst. Solids* **16** (1974) 325.
20. J.H. Wendorf & E.W. Fischer: *Kolloid Z.u.Z. Polymere* **251** (1973) 876.
21. J. Zarzycki & R. Mezard: *Phys. Chem. Glasses* **3** (1962) 163.
22. T.P. Seward & D.R. Uhlmann: In *Amorphous Materials* (Giley, 1971).
23. R.L. Mozzi & B.E. Warren: *J. Appl. Cryst.* **2** (1969) 251.
24. F.M. Dunlevy & A.R. Cooper: In *Structure of Non-Cryst. Mat.* (1976).
25. D.R. Uhlmann: *J. Non-Cryst. Solids* **25** (1977).
26. W.H. Zachariasen: *J. Am. Chem. Soc.* **54** (1932) 1861.
27. P.J. Flory: *Principles of Polymer Chemistry* (Cornell Univ. Press., 1953).
28. G.S.Y. Yeh: *Crit. Revs. Macromol. Sci.* **1** (1975).
29. R.G. Kirste, W.A. Kruse & K. Theil: *Polymer* **16** (1975) 120.
30. G.D. Wignall & G.W. Longman: *J. Mat. Sci.* **3** (1973) 1419.
31. A.L. Renninger, G.G. Wicks & D.R. Uhlmann: *J. Polymer Sci.-Phys. Ed.* **15** (75) 1247.
32. G. Patterson: *J. Macromol. Sci.-Phys.* **B12** (1976) 27.

## **Electron Microscopy and SAXS Studies of Amorphous Polymers**

**BY D. R. UHLMANN**

**Department of Materials Science and Engineering,  
Massachusetts Institute of Technology,  
Cambridge, Massachusetts, U.S.A.**

Reprinted from

**FARADAY DISCUSSIONS  
OF  
THE ROYAL SOCIETY OF CHEMISTRY**

**No. 68**

**FARADAY DISCUSSIONS 68**

**1979**

# Electron Microscopy and SAXS Studies of Amorphous Polymers

By D. R. UHLMANN

Department of Materials Science and Engineering,  
Massachusetts Institute of Technology,  
Cambridge, Massachusetts, U.S.A.

Received 7th June, 1979

Small angle X-ray scattering (SAXS) and high resolution electron microscopy have been used to characterize the structure of glassy polymers. The SAXS from polycarbonate, poly(methyl methacrylate), poly(ethylene terephthalate), poly(vinyl chloride) and polystyrene is inconsistent, both in the form and magnitude of the scattered intensity, with the presence of nodules as representative of the bulk structure. The electron microscope results provide no evidence for heterogeneities on a scale and volume fraction of the reported nodules. Only the pepper and salt features characteristic of microscope operation near the resolution limit are seen. It is suggested that the structures of these amorphous thermoplastics be regarded as random arrays.

## 1. INTRODUCTION

The question of local order in nominally glassy polymers has been the subject of considerable controversy during the past decade. A sizeable number of investigations, based primarily on electron microscope observations, have cast doubts upon the utility of the random coil model for representing the structure of these polymers. The results of the investigations are well summarized in ref. (1) and (2).

The essential and initially surprising feature of these results has been the observation of heterogeneities, typically on a scale of  $\approx 50\text{-}100 \text{ \AA}$ , in a number of polymers. Among the polymers in which such nodular structures have been observed are polycarbonate, poly(ethylene terephthalate), natural rubber, isotactic and atactic polystyrene, poly(vinyl chloride), and poly(methyl methacrylate). Investigations of nodular structures have included the following types of observations: (1) the nodular structures have been observed in both direct transmission and replication electron microscopy; (2) dark-field electron microscopy has indicated the presence of ordered regions of approximately the same size as the nodular regions; (3) the nodular structures have been observed to change with changes in the process history of the samples; in particular, they have been observed to increase in size and/or rearrange upon annealing and to align upon stretching; in some cases, the nodules have been suggested to merge on annealing into patches, which in turn aggregate to form lamellar crystalline structures; (4) when etched by ion bombardment, glassy polymers do not thin down uniformly; some at least develop a granularity on the scale of the nodular structures; (5) the size of the nodules varies from one polymer to another, but does not differ significantly from one form of a given polymer to another (as isotactic *vis-à-vis* atactic); and (6) at least in the case of polystyrene, electron irradiation has a pronounced effect on a diffraction halo corresponding to a Bragg law *d*-spacing which is identified as corresponding to an intermolecular rather than an intramolecular distance.

## 88 ELECTRON MICROSCOPY AND SAXS STUDIES OF AMORPHOUS POLYMERS

The accumulated weight of these observations has been taken as strong evidence against the random coil model for representing the structure of glassy polymers and support for the existence of regions of local order in the materials. Electron microscope studies of thermosetting polymers such as epoxy resins<sup>3</sup> have indicated heterogeneities on similar scales to those seen in glassy thermoplastics. In these cases, the technique of replication electron microscopy was employed; and the form and scale of the structures were found not to depend on the curing conditions.

In addition to such direct observations of heterogeneities in nominally glassy polymers, a number of measurements, ranging from X-ray diffraction to mechanical relaxation, have been taken as inconsistent with the random network model. In addition to the work discussed in ref. (1), particular note should be made of the relaxation data obtained on amorphous polystyrene using a torsional braid technique.<sup>4</sup> Such data have indicated a transition occurring at temperatures above the glass transition temperature,  $T_g$ . Such transitions have been termed  $T_{11}$  transitions, and taken by some workers as evidence for local order in the polymers in their glassy state.

In contrast to these suggestions of local order in the materials, many properties of amorphous thermoplastics are well described by the random coil model. Many of the results of relevance here were reviewed by Flory.<sup>5</sup> In addition to these, the results of studies using small angle neutron scattering<sup>6</sup> and wide angle X-ray scattering<sup>7</sup> have provided important insight into the structure of amorphous polymers. These will be considered by others at the present Discussion, and discussed briefly in section 4 below.

The present paper will describe small angle X-ray scattering (SAXS) and electron microscopy studies of a number of amorphous thermoplastics. It will also present results of SAXS studies of cured epoxy resins. Some of the results have been reported previously;<sup>8,9</sup> the interested reader is referred to these papers for details, where appropriate, which are omitted here.

### 2. SAXS STUDIES

SAXS data on polycarbonate (PC), poly(methyl methacrylate) (PMMA), poly(ethylene terephthalate) (PET), poly(vinyl chloride) (PVC), polystyrene (PS) and a number of cured epoxy resins were obtained using a Bonse-Hart SAXS system. The system incorporates slotted germanium single crystals in both the incident beam and diffracted beam in order to eliminate the effects of slit-width smearing while still maintaining usable intensities. After correcting for background and absorption, the data were desmeared using a weighting function which was determined experimentally.<sup>9</sup> In accomplishing this desmearing, an iterative deconvolution procedure was employed, using a multiplicative correction to obtain the trial function at each step. This has been taken as the lower limit of the present measurements.

In carrying out the desmearing procedure, it was assumed that the scattering from the specimens was isotropic. This assumption was verified experimentally by rotating the specimen and investigating the effect on the scattered intensity. The intensity was found not to change upon sample rotation.

The measured intensities, corrected for background and absorption and desmeared, were placed on an absolute basis by comparison with the scattering measured for a known standard material, obtained under similar diffraction conditions. In all cases, a colloidal silica suspension (Du Pont Ludox IBD 1019-69) diluted to 1.46 % by volume was used for this purpose.

For all the glassy thermoplastics, samples of commercial materials were employed (Lexan, Plexiglas G, PET from Du Pont chill roll, American Hoechst PVC, and lens-

grade PS). The epoxy resins included EPON 828 cured with triethylene tetramine (TETA) for 4 days at 100 °C; EPON 828 cured with nadicmethyl anhydride (NMA) and benzylidimethyl amine (BDMA) for 14 days at 175 °C; and EPON 812 cured with dodecenylsuccinic anhydride (DDSA) together with NMA and BDMA for 24 h at 130 °C.

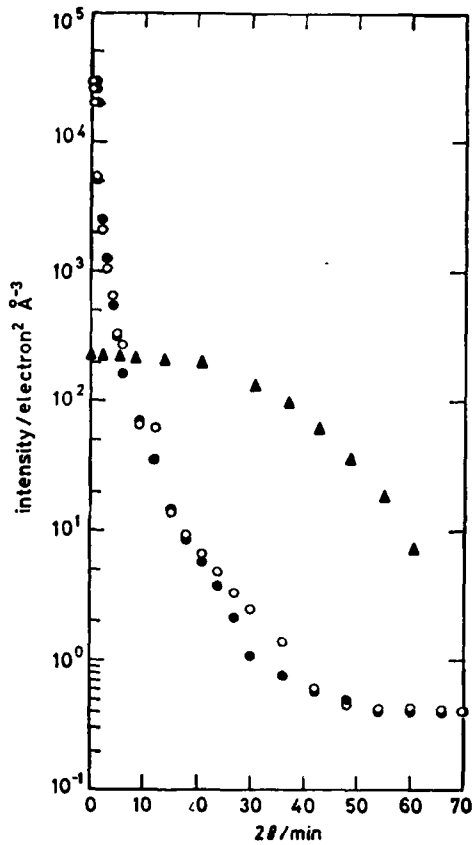


FIG. 1.—Variation of absolute SAXS intensity with scattering angle for amorphous PET: ○, de-smeared experimental data; ●, calculated intensity for thermal density fluctuations + distribution of heterogeneities; ▲, calculated intensity for a 50 vol. % concentration of 100 Å heterogeneities characterized by the crystal excess density.

Representative results obtained on the amorphous thermoplastics are shown in fig. 1 and 2 for glassy PET and PVC, respectively. For these and all the other glassy polymers, the intensity decreases markedly with increasing scattering angle at very small angles and reaches or approaches a nearly constant value over a range of intermediate small angles.

A nearly constant (asymptotic) SAXS intensity at small diffraction angles ( $2\theta < 1^\circ$ ) is expected for thermal fluctuations in density in an otherwise homogeneous material such as an ideal liquid or glass. In the case of glasses, Weinberg<sup>10</sup> has suggested that the configurational fluctuations (but not the vibrational fluctuations) present in the liquid at the glass-transition temperature,  $T_g$ , should be retained in the

glassy material. The magnitude of the asymptotic zero-angle scattering may then be expressed as:

$$I(0) = V \langle (\Delta\rho)^2 \rangle = kT_g K_T(T_g) \rho^2 \quad (1)$$

here  $K_T(T_g)$  is the isothermal compressibility at  $T_g$ ;  $k$  is Boltzmann's constant;  $\rho$  is the average electron density; and  $\langle (\Delta\rho)^2 \rangle$  is the mean-square density fluctuation in a region of volume  $V$ .

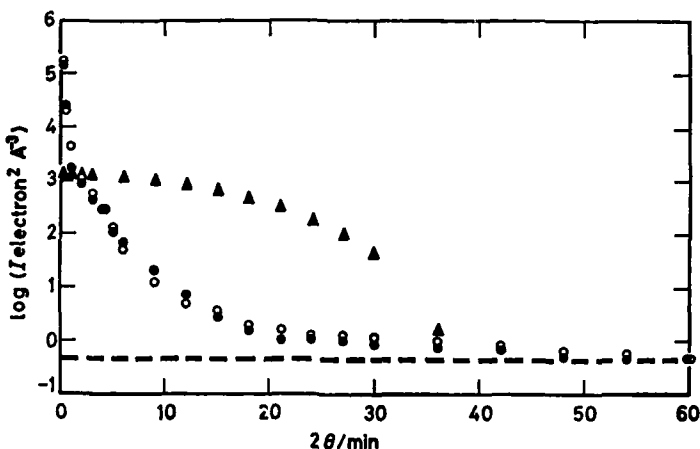


FIG. 2.—Variation of absolute SAXS intensity with scattering angle for PVC: ●, desmeared experimental data; ○, calculated intensity for frozen-in thermal density fluctuations plus scattering from heterogeneities listed in table 1; ▲, calculated intensity from heterogeneities 200 Å in diameter, having the crystal excess density, and occupying 50% by volume; (—), intensity due to thermal density fluctuations.

For each of the glassy thermoplastics, the measured SAXS intensity reaches or approaches an asymptotic value which is close to that predicted for thermal density fluctuations frozen-in at the glass transition. (The difference between the measured and predicted intensities varies from < 10% of the predicted value for PC to  $\approx 50\%$  for PMMA). Considering the possible uncertainty in the values used for the high temperature compressibility, the agreement here must be regarded as impressive.

The occurrence of scattering in the very small angle region above the level corresponding to thermal density fluctuations indicates the presence of heterogeneities in the material. Using the exact expression for the SAXS from spheres, distributions of heterogeneities such as those shown in table 1 for PVC were obtained by fitting the experimental data. The points labelled by open circles in fig. 2 show the scattering from the particles in table 1 superimposed on that from thermal density fluctuations. The agreement between measured and calculated intensities is seen to be excellent; and comparable agreement could be obtained for each of the other polymers investigated.

In estimating the actual concentrations of the heterogeneities which are indicated by the increase in SAXS intensity at very small angles, it is necessary to assume a value for the density difference  $\Delta\rho$  between heterogeneities and matrix. In the case of PET, for example, if the scattering is assumed to be associated with microvoids with a density difference from the matrix equal to the bulk density,  $(\Delta\rho)^2 = 0.20 \text{ electron}^2 \text{ Å}^{-6}$ , the values of  $C(\Delta\rho)^2$  obtained from fitting the experimental data would indicate

volume concentrations of  $(4 \times 10^{-6})$ - $(2 \times 10^{-5})$ , and the total concentration of heterogeneities estimated from the intensity invariant (see below) would correspond to a volume fraction of  $\approx 7 \times 10^{-5}$ . If, in the more likely case for this material, the scattering is associated with crystallites, with a density difference from the matrix of  $(\Delta\rho)^2 = 2 \times 10^{-3}$  electron $\text{Å}^{-6}$ , the values of  $C(\Delta\rho)^2$  would indicate volume concentrations of 0.04-0.2 %. The total concentration of heterogeneities estimated from the intensity invariant in this case would correspond to a volume fraction of  $\approx 0.7 \%$ . Even smaller total concentrations of heterogeneities were estimated for PC and PMMA.

TABLE I.—SIZES AND CONCENTRATIONS OF HETEROGENEITIES DESCRIBING THE SAXS FROM PVC

radius/ $\text{\AA}$	$C(\Delta\rho)^2/10^7$ electron $\text{\AA}^{-6}$	$C/\%$ ( $\Delta\rho \approx 0.034$ electron $\text{\AA}^{-3}$ )	$C/\%$ ( $\Delta\rho = 0.45$ electron $\text{\AA}^{-3}$ )
4500	5.78	0.05	0.000 29
3500	2.89	0.025	0.000 14
2000	1.33	0.0115	0.000 066
1000	1.91	0.0165	0.000 094
700	3.24	0.028	0.000 16
500	15.0	0.13	0.000 74
150	8.44	0.073	0.000 42
50	23.1	0.20	0.000 14

A check on the estimated concentrations of heterogeneities can be obtained by evaluating the contribution of the heterogeneities to the mean-square density fluctuations,  $\langle(\Delta\rho)^2\rangle$ . The magnitude of this quantity for the scattering above that due to thermal density fluctuations may be determined from the invariant integral:

$$\int_0^\infty h^2 I'(h) dh = 2\pi^2 \langle(\Delta\rho)^2\rangle \quad (2)$$

where  $I'(h)$  is the intensity above that due to thermal density fluctuations. In all cases, the magnitude of  $\langle(\Delta\rho)^2\rangle$  determined in this way is close to the sum of the contributions from the heterogeneities inferred from fitting the intensity data.

In the case of PVC, table I shows the concentrations which are implied by assuming the crystal excess density ( $\Delta\rho = 0.034$  electron $\text{\AA}^{-3}$ ) and also those implied by assuming that the heterogeneities are microvoids ( $\Delta\rho = 0.45$  electron $\text{\AA}^{-3}$ ). It is important to note the concentration of very small (50  $\text{\AA}$ ) particles in the indicated distribution. The inclusion of these particles 50  $\text{\AA}$  in radius serves two purposes. First, it helps to account for the measured intensity in excess of the thermal fluctuation scattering at angles between 20 and 30 min, and it accounts for the slight negative slope observed for this part of the curve. Second, it is needed to make up the difference in the mean-square fluctuation density which the larger particles cannot represent by themselves.

It should be noted that particular distributions of heterogeneities, such as that shown in table I, are by no means unique. Other models with somewhat different values for the sizes and relative contributions could undoubtedly provide an equivalent description of the experimental data. Any such model must, however, associate the scattering at very small angles with small concentrations of rather large particles (as concentrations in the range of 0.04 vol % of particles several thousand  $\text{\AA}$  in diameter in the case of PC).

Any implication that the heterogeneities are characterized by the crystal excess density is not intended; and it seems likely that many of the heterogeneities are not

characterized by such a difference in density relative to the matrix. In particular, it seems reasonable that the larger heterogeneities are not large crystals but rather are heterogeneities extrinsic to the polymer (such as dirt or perhaps stabilizers or processing aids which have precipitated during processing). These should have a larger  $\Delta\rho$  than crystallites, and would be present in concentrations smaller than those indicated for heterogeneities with the crystal excess density.

It is also possible that the heterogeneities are characterized by  $\Delta\rho$  values which are smaller than the crystal excess density, in which case the volume fractions would be larger. For PVC with  $\Delta\rho = 0.0045$  electron  $\text{\AA}^{-3}$  ( $\Delta\rho/\rho = 1\%$ ), for example, the indicated concentration of 500  $\text{\AA}$  heterogeneities would be  $\approx 7\%$ . Such heterogeneities could represent locally dense regions containing relatively high concentrations of chain entanglements, probably given some permanence by the presence of a small concentration of small crystallites.

The forms of the scattering expected for heterogeneities having the size of the nodules reported in electron microscope studies, occupying a volume fraction of 50% and characterized by the crystal excess density are shown by the filled triangles in fig. 1 and 2. It is seen that the experimental data are inconsistent, both in the form and magnitude of the scattered intensity, with the scattering expected for such an assemblage of nodules.

Use of the invariant integral to estimate the mean square density fluctuation in the materials, beyond that expected for thermal density fluctuations, also presents problems for the nodule hypothesis. In particular, density differences between heterogeneities and matrix in the range of 1% or less of the bulk density are indicated. Such small density differences would not produce perceptible contrast in the electron microscope, either by amplitude contrast or by Fresnel type phase contrast; and it seems unlikely that heterogeneities differing from the amorphous density by as little as 1% could be characterized by sufficient order that perceptible diffraction contrast would be noted.

Taken *in toto* the SAXS results provide strong evidence that the nodular structures seen in the electron microscope are highly unlikely to be representative of the bulk structure. It is suggested, therefore, that the nodules may be associated with surface effects, and that the structures of the polymers be regarded as random amorphous arrays, with small concentrations of heterogeneities superimposed on thermal density fluctuations frozen-in at the glass transition.

While most of the controversy surrounding the existence of nodules has centred about thermoplastic polymers, many studies have been conducted on network-forming thermosetting polymers as well. Heterogeneities, generally on a scale of 50-3000  $\text{\AA}$  and present in large volume fractions, have been observed in transmission electron microscope studies of a number of cured epoxy resins. Among such studies, that of Racich and Koutsky<sup>3</sup> has provided the most clear-cut evidence for the presence of structural inhomogeneities. These workers observed heterogeneities (which they termed nodular structures) on free surfaces, fracture surfaces and etched surfaces of epoxy resins of widely different cures and chemistries.

The SAXS intensity from the three cured epoxy resins are illustrated by the data in fig. 3 for the Epon 812/NMA/DDSA material. The intensity is seen to decrease with increasing scattering angle out to  $\approx 24^\circ$ , beyond which the intensity remains almost constant. The asymptotic level of scattering is close to that expected for thermal density fluctuation (0.3 electron<sup>2</sup>  $\text{\AA}^{-3}$  as compared with 0.18 electron<sup>2</sup>  $\text{\AA}^{-3}$ ).

The pronounced rise in scattered intensity at small angles ( $2\theta < 24^\circ$ ) and the excess asymptotic scattering at larger angles (over that predicted by fluctuation theory) can be associated with heterogeneities in the sample. The sizes and concentrations of heterogeneities needed to describe the observed scattering are shown in table 2. The

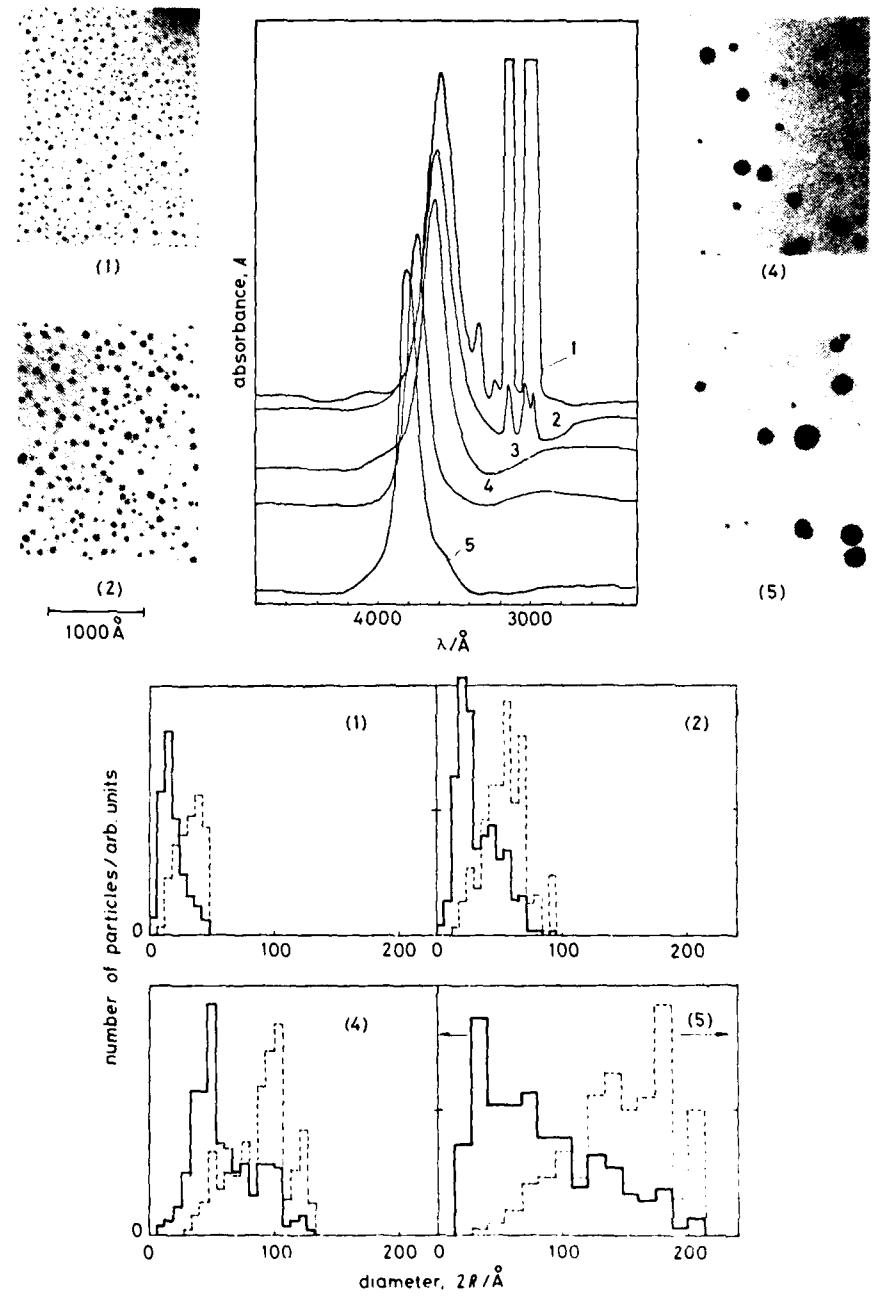


FIG. 5. Optical absorption spectra of silver microcrystallites in argon matrices produced by the gas aggregation technique as a function of crystallite size, the corresponding micrographs and size distribution histograms. (—) Number distribution, (---) mass distribution

[To face page 92]

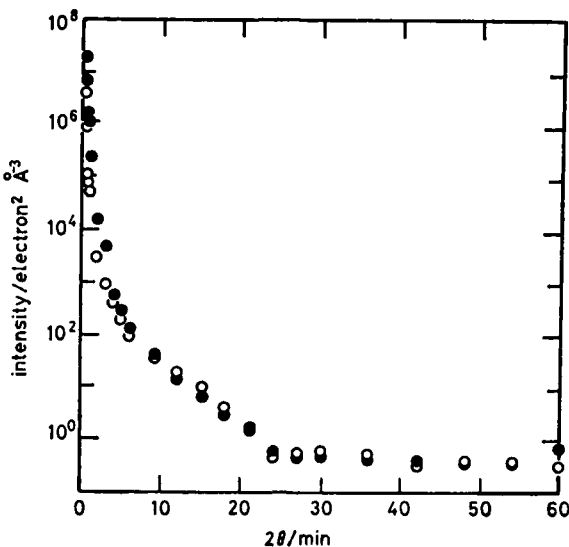


FIG. 3.—Variation of absolute SAXS intensity with scattering angle for Epon 812/NMA/DDSA: ●, desmeared experimental data; ○, calculated intensity for thermal density fluctuations + distribution of heterogeneities shown in table 2.

presence of large heterogeneities ( $R > 250 \text{ \AA}$ ) is required to explain the large increase in intensity at very small angles. It is likely that these heterogeneities are extrinsic to the polymers. While adventitious impurities such as dirt may be responsible for some of this scattering, the most likely source is gas (air) bubbles incorporated in the resin during its cure. As seen in table 2, concentrations of gas bubbles in the range of  $10^{-5}$  are sufficient to account for the observed scattering (above fluctuation scattering) in the very low angle region.

TABLE 2.—CALCULATED SIZES AND CONCENTRATIONS OF HETEROGENEITIES IN EPOX 812/NMA/DDSA<sup>10</sup>

$R/\text{\AA}$	$c(1 - c)(\Delta\rho)^2$	$c(\Delta\rho = 1\%)$	$c(\Delta\rho = 10\%)$	$c(\Delta\rho = 100\%)$
150	$3.18 \times 10^{-6}$	0.266	$1.95 \times 10^{-3}$	$1.95 \times 10^{-5}$
500	$1.91 \times 10^{-6}$	0.135	$1.17 \times 10^{-3}$	$1.17 \times 10^{-5}$
3000	$1.77 \times 10^{-6}$	0.124	$1.08 \times 10^{-3}$	$1.08 \times 10^{-5}$
5000	$9.55 \times 10^{-6}$	— <sup>a</sup>	$5.88 \times 10^{-3}$	$5.88 \times 10^{-5}$
6000	$5.53 \times 10^{-6}$	— <sup>a</sup>	$3.38 \times 10^{-3}$	$3.38 \times 10^{-5}$

<sup>a</sup> Gives  $c(1 - c) > 0.25$ .

The scattering at larger angles (still in the small angle region) is associated with smaller heterogeneities. The excess scattering (above that due to thermal fluctuations) indicates the presence of small ( $< 100 \text{ \AA}$ ) inhomogeneities in the materials. Again, concentrations of gas bubbles in the range of  $10^{-5}$  would be sufficient to account for the observed excess scattering, although the presence of other structural inhomogeneities could also account for the scattering. If the densities of these heterogeneities differ only slightly from that of the matrix (as  $\Delta\rho/\rho = 1\%$ ), they could be present in sizeable concentrations.

For electron microscope studies carried out using direct transmission on thin sections, heterogeneities in a  $1000 \text{ \AA}$  thick sample of epoxy would provide discernible

## 94 ELECTRON MICROSCOPY AND SAXS STUDIES OF AMORPHOUS POLYMERS

contrast only if they differed in density from the bulk by  $\approx 5\text{-}10\%$ . Examination of table 2 shows, however, that heterogeneities differing from the bulk density by 10% or more can only be present at concentrations in the range  $\approx 0.1\%$ , a range which is much smaller than the concentrations indicated for the nodular features.

For studies carried out using electron microscopy of surface replicas, which represent the largest fraction of the observations of nodular features in epoxy resins, a different question is posed by the present results. The volume fractions of heterogeneities seen in the electron microscope studies are consistent with the SAXS results only if they differ in density by perhaps 1% or less from the bulk. In light of the modest differences in density between cured and uncured epoxy resins, differences in density of 1% or less in the cured resin seem not unreasonable. It remains to be established, however, how regions with such differences in density become visible on fracture surfaces. Certainly there is good reason for expecting regions of different crosslink density in cured epoxy resins. What remains to be clarified is the relation between such regions and the features seen in electron microscope studies. The present SAXS results should be viewed as providing data with which any proposed structural model must be consistent.

### 3. ELECTRON MICROSCOPE STUDIES

The SAXS results discussed in the preceding section cast strong doubts on the validity of the electron microscope observations which suggested the occurrence of nodular structures as essential features of amorphous polymers. It seemed highly desirable, therefore, to re-examine the structure of glassy polymers using the technique of high-resolution electron microscopy.

Appropriately thin samples of PC, PET, PVC and PS were cast from solutions using the same techniques as employed by previous investigators; the specimens were viewed in both bright- and dark-field using a high resolution electron microscope which provided magnifications of 500 000 $\times$  or more on the photographic plates when desired.

For all four polymers, the structures were seen to be featureless down to the limit of resolution of the electron microscope. Only the "pepper and salt" structure characteristic of electron micrographs taken at high resolution is seen. The "pepper and salt" structure observed is a result of the use of a finite objective aperture to limit the amount of information (in the form of transmitted or scattered electrons) from the object that is used to construct the image. If the object is considered to be an array of atoms or molecules, then the convolution of the object with an Airy disc (the aperture transform) will yield a blurred image of the array observed as the "pepper and salt" structure.

No evidence was found in either bright-field or dark-field for nodular features as reported by others. The combination of featureless bright-field and dark-field micrographs provides strong evidence for a highly homogeneous structure. Since PET was the first polymer for which distinct nodular structures in the glassy state were reported, and since the nodules in this material appear with greater clarity than those in other polymers, it was decided to subject PET to even closer scrutiny. Several through-focus series of micrographs were taken, a representative set of which is shown in fig. 4. This series shows the absence of perceivable structure in the in-focus micrograph, and illustrates how apparent structure can be developed in the micrographs by going to either an underfocus or an overfocus condition. The change in the scale of the "salt and pepper" noted with change in focus can be considered as an additional defocus convolution with the original object.

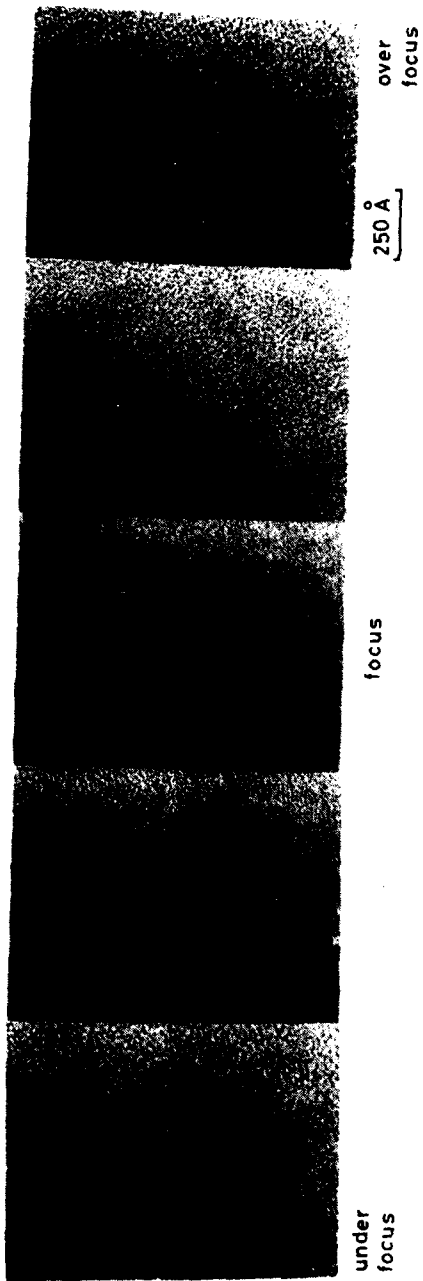


FIG. 4. - Through-focus series of electron micrographs of PET showing the absence of structural features when in focus and the development of apparent structural features when out of focus.

[To face page 94]

These results suggest that the fine-scale ( $<20 \text{ \AA}$ ) apparent structure seen in some previous investigations may simply reflect the use of electron microscopes of insufficient resolution, or may result from the lack of proper focus in taking the micrographs. Neither of these possibilities can be confirmed at present nor can alternative explanations based on other effects, such as radiation damage from the electron beam or the possibility that the observed nodules represent surface features of the polymers.

#### 4. GENERAL DISCUSSION

The combined results of the SAXS and electron microscope studies suggest that nodular features should not be taken as representative of the bulk structure of thermoplastic polymers. These findings are in accord with the results of recent light scattering and small angle neutron scattering (SANS) investigations of glassy polymers. Among the former, Patterson<sup>11</sup> investigated the effects of cooling on light scattering from PMMA and PC. No evidence was found for an increase in the number density or size of heterogeneities in the polymers as the temperature was lowered, as would be expected for nodular structures as regions of local order.

Among the SANS studies, that of Benoit<sup>12</sup> can be taken as representative. The radii of gyration of eight molecular weight polystyrene polymers were found to be the same, within experimental error, as those of the polymers in a theta solvent (where the random coil is widely acknowledged as providing a useful representation of the chain conformation).

The combined weight of all these studies, together with those cited in ref. (5), leads to the conclusion that the structure of amorphous thermoplastics should be represented by random array models such as the random coil, rather than by models such as the nodule hypothesis, whose essence involves regions of locally high order. When examined in detail, all the evidence advanced in support of such local-order models seems subject to question. Even the observation of  $T_{11}$  transitions seems to involve the interaction of the liquid with the braid on which it is supported, and cannot be taken as unequivocal support for regions of local order. It is suggested, therefore, that the controversy be laid to rest, and that attention be directed to more fruitful areas such as the structural changes involved in crystallization and the structural differences between surfaces and bulk material.

AFASP-77-3226

Financial support for the present work was provided by the U.S. Air Force Office of Scientific Research. This support is gratefully acknowledged, as is the previous support of the National Science Foundation. The direct contributions of Drs. Renninger, Wicks, Straff and Vander Sande, as well as Mr. Matyi and Miss Meyer, made this presentation possible.

<sup>1</sup> G. S. Y. Yeh, *Crit. Rev. Macromol. Chem.*, 1972, **1**, 173.

<sup>2</sup> P. H. Geil, *Morphology of Amorphous Polymers*, Final Report USAROD, Contract DAHCO4-70C-0032.

<sup>3</sup> J. L. Racich and J. A. Koutsky, *Bull. Amer. Phys. Soc.*, 1975, **20**, 456.

<sup>4</sup> J. K. Gillham and R. F. Boyer, *J. Macromol. Sci. Phys.*, 1977, **B13**, 497.

<sup>5</sup> P. J. Flory, *J. Macromol. Sci. Phys.*, 1976, **B12**, 1.

<sup>6</sup> D. G. H. Ballard, G. D. Wignall and J. Schelten, *Europ. Polymer J.* 1973, **9** 965.

<sup>7</sup> G. D. Wignall and G. W. Longman, *J. Mater. Sci.*, 1973, **8**, 1439.

<sup>8</sup> A. L. Renninger, G. G. Wicks and D. R. Uhlmann, *J. Polymer Sci. Phys.*, 1975, **13**, 1247.

<sup>9</sup> M. Meyer, J. Vander Sande and D. R. Uhlmann, *J. Polymer Sci. Phys.* 1978, **16**, 2005.

<sup>10</sup> D. L. Weinberg, *Phys. Letters* 1963, **7**, 324.

<sup>11</sup> G. Patterson, *J. Macromol. Sci. Phys.*, 1976, **B12**, 61.

<sup>12</sup> H. Benoit, *J. Macromol. Sci. Phys.*, 1976, **B12**, 27.

#### POLYMER GLASSES AND OXIDE GLASSES

D. R. Uhlmann  
Department of Materials Science and Engineering  
Massachusetts Institute of Technology  
Cambridge, Massachusetts  
U.S.A.

The similarities and differences in the structure of polymer glasses and oxide glasses are reviewed, together with models suggested to describe structure on various scales. It is suggested that random array models seem to provide the best description of structure for most glasses of both types of materials. Also considered are the crystallization and viscous flow behavior of both classes of materials, together with the implications of the observed behavior for their formation as amorphous solids. The role of the chain character of polymer liquids in affecting their kinetic behavior is considered, as are recent controversies concerning the microstructure of partly-crystallized polymers.

#### INTRODUCTION

The oldest known glasses are the FeO-alkaline earth-aluminosilicates returned from the lunar surface, which have persisted in the glassy state for periods in the range of a billion years. The first commercial glasses, of much more recent origin, were also silicate glasses; and such glasses represent the dominant part of the glass industry to the present day. Prior to the twentieth century, when one spoke of glass, he referred to amorphous solids, generally comprising silicates containing alkali and alkaline earth oxides, which were prepared by melting at high temperature followed by cooling from the liquid state.

During the past 80 years, it has been found that glass formation is not restricted to silicates, nor even to inorganic oxides. Rather, glasses have been formed of a wide range of materials, including polymers, salts, simple organics, water, chalcogenides, and even metals. The techniques for forming glasses also cover a very wide range, including splat cooling and laser film melting, evaporation sputtering, ion implantation, thermal and anodic oxidation, chemical vapor deposition, electrodeposition, hydration of gels, and exposure to radiation or shock waves. The varieties of techniques used to form glasses have recently been summarized by Scherer and Schultz (1980), and will be discussed by Sakka (1980) at this Conference.

The ease of glass formation on cooling a liquid ranges from  $B_2O_3$ , which has never been crystallized from a dry melt at atmospheric pressure; atactic polymers, which cannot crystallize because of configurational constraints; and albite ( $NaAlSi_3O_8$ ) which has been held for more than a year at considerable undercoolings without observable crystallization; through the familiar silicate glasses of industry which can be formed as amorphous solids on a scale of inches but not feet, and materials such as polyethylene terephthalate which will partially crystallize in bodies of even 1/8 inch thickness unless cooled rapidly; to materials which crystallize unless cooled with great rapidity, including the widely-investigated metal alloy glasses whose formation requires cooling rates in the range

$10^6 \text{ K sec}^{-1}$ , and which can therefore be prepared as glasses only when at least one dimension is small.

The present paper will be concerned with the two types of glasses of greatest technological importance, oxide glasses and polymer glasses. Specific attention will be directed to the structural features of both types of glasses, to models used to represent the structures, and to the kinetic processes important in their viscous flow and crystallization behavior which affect their ability to be formed as glasses.

The thesis will be advanced that developments in both of these areas have in many respects proceeded along parallel lines, with regrettably little interconnection between them, and with regrettably little communication between workers dealing with the two classes of materials. It is hoped that Conferences such as the present one, bringing together workers from a variety of disciplines will promote increased interaction and interconnection during the coming decades.

#### MODELS OF GLASS STRUCTURE

Among the models used to represent the structure of glasses, the following have received widest attention. In each case, reference will be made to the earliest or the classic descriptions of the structure, with examples chosen from both polymer and oxide glasses. It will be seen that models based on the same conceptualization have been advanced to represent both type of glasses, apparently independently.

#### Crystallite Models

X-ray diffraction patterns of glasses generally exhibit broad peaks centered in the range in which strong peaks are also seen in the diffraction patterns of the corresponding crystals. This is shown in Fig. 1 for the case of  $\text{SiO}_2$ . Such observations led to the suggestion that glasses are composed of arrays of very small crystals, termed crystallites. The observed breadth of the diffraction pattern of the glass was suggested to result from particle-size broadening, which occurs for sizes of coherently diffracting arrays smaller than about  $0.1 \mu\text{m}$ . In the case of oxides, this model was applied to both single-component and multi-component glasses, with the structure in the latter case being viewed as composed of crystallites of compositions corresponding to compounds in the particular system. In the case of oxide glasses, this model is most frequently associated with Porai-Koshits (e.g., Valenkov and Porai-Koshits, 1936). Variations of this model have been used by many others in the field of oxide glasses. In the case of polymer glasses, the model has received much less attention; although evidence for regular inter-chain correlations has been suggested by several investigators,

#### Random Array Models

According to random array models, glasses are viewed as three-dimensional arrays, lacking symmetry and periodicity, in which no unit of the structure is repeated at regular intervals in three dimensions. In the case of oxide glasses, the suggested random arrays were networks of oxygen polyhedra, and the model is known as the random network model. This model is most frequently associated with names of Warren (1937) and Zachariasen (1932).

Adopting the hypothesis that a glass should have an energy content similar to that of the corresponding crystal, Zachariasen suggested four rules for the formation of an oxide glass. These are:

1. Each oxygen ion should be linked to not more than two cations.

2. The coordination number of oxygen ions about the central cation must be small ( $\leq 4$ ) or less.
3. Oxygen polyhedra share corners, not edges or faces.
4. At least three corners of each polyhedron should be shared.

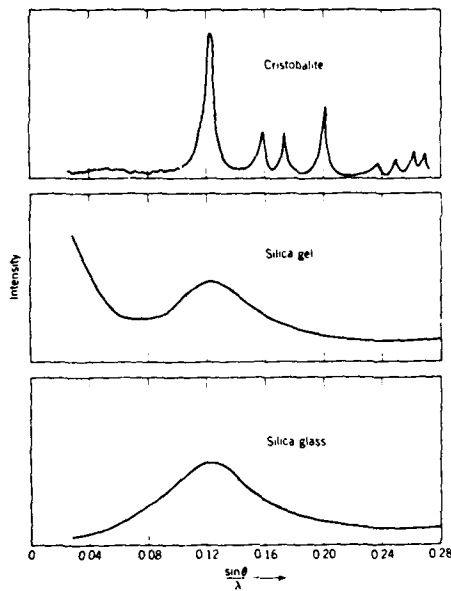


Figure 1  
X-ray diffraction patterns from cristobalite, silica gel and vitreous silica.  
After Warren and Biscoe (1938).

In practice, the glass-forming oxygen polyhedra are triangles and tetrahedra, and cations forming such coordination polyhedra have been termed network formers. Ions such as the alkalis and alkaline earths, which provide additional oxygen ions to the structure and modify the character of the network, are termed network modifiers.

Although it is now recognized that the similarity in internal energy between liquid and crystal is not a critical factor in glass formation (see below), the structural model advanced on this basis has, as we shall see, rather wide applicability.

Modification of the model is, of course, required for regions of composition where the formation of a three-dimensional network is not possible--e.g., the regions of the metasilicate compositions in alkali silicate systems where even the crystals are composed of chains of  $\text{SiO}_4$  tetrahedra, or the exciting new classes of oxide

glasses produced by rapid quench techniques in which network formation is unlikely (Georgy, Gyorgy et al., 1979). For such materials, the generalized picture is that of a random array in which the structural elements are randomly arranged and in which no unit of the structure is repeated at regular intervals.

Such a generalization is necessary in the case of linear polymers, which consist of long-chain molecules, where specific consideration must be directed to the chain character of the materials. The most forceful proponent of the random array model for the structure of amorphous polymers has been Flory (e.g., Flory, 1953). The structural features of the random coil model have been considered by Flory in his talk at this conference.

The essential and striking features of this model are Flory's suggestions that the chain conformations in the melt are to a good approximation unperturbed by the presence of neighboring chains and that the configurations in the molten or glassy polymer are similar to those in a dilute solution. Such a model has been picturesquely portrayed as a tangled bowl of sticky spaghetti or a barrel packed with wiggling eels.

The random coil model has been applied to a variety of flexible-chain polymers, which represent the great majority of the polymers of commerce and include materials ranging from natural rubber and polystyrene to polymethyl methacrylate and polycarbonate.

It was recognized that the random coil model would not be appropriate to represent the structure of rigid-chain polymers such as the alpha-helical polypeptides or the polyparabenzimidest and the same Flory (1956) presented the basic theoretical treatment for solutions of rigid-chain macromolecules. While such polymers are beyond the focus of the present paper, it should be noted that they represent an exciting new class of materials, as exemplified by the Kevlar fibers of duPont, whose investigation offers particular promise. Such rigid-chain molecules are notable for the formation of liquid-crystalline arrays in melt or solution.

#### Micelle and Nodule Models

According to these models, glasses are composed of structural features characterized by a degree of order intermediate between that of a perfect crystal and a random array. The degree of order in the characteristic features is suggested to be large enough for their mutual misorientation to be discerned in an electron microscope, yet small enough that sharp Bragg reflections are not seen in X-ray diffraction patterns. In the case of oxide glasses, these features were termed micelles. They were advanced to account for the heterogeneities on a scale of about 100 Å observed in electron microscope studies of single-component glasses such as SiO<sub>2</sub> and  $\text{Ca}_2\text{SiO}_5$  (see, e.g., Zarzycki and Mezard, 1962).

Electron microscope observations of glassy polymers, carried out a few years later, indicated the presence of heterogeneities on a similar scale to that seen in oxide glasses (90-200 Å), present in similarly high volume fractions (in the range of 50%). Similar models were advanced to represent the structure. The features with an intermediate degree of order were termed nodules. Such models are most closely associated with Geil (1975) and Yeh (1972).

#### Paracrystal Models

The term paracrystallinity was introduced by Hosemann (see Hosemann and Bagchi, 1962) to represent structural features whose order can be described as a sort of "propagation of errors" from that of a perfect crystal. The propagation of errors in packing sets limits to the scale on which sensible order can occur; and such models, originally used to describe the structure of partly-crystalline polymers,

have been extended to represent the structure of nominally-glassy polymers. In particular, the notion of paracrystallinity can be taken to provide a specific embodiment of the approach suggested by the micelle or nodule views of glass structure.

#### Structural Models Based on Five-Fold Symmetries

The existence in liquids of nearly regular coordination polyhedra which cannot fill space was suggested by Frank (1952) and Bernal (1959). In both cases, structural elements having five-fold symmetry were emphasized; and, indeed, the symmetry of the coordination cells observed in hard sphere models of liquids is predominantly pentagonal. In one view, the existence of such structures was related to the suggestion that the energy of a molecular group may be lower for some forms of the coordination polyhedra which do not fill space than for any space-filling form. According to another view, the stabilizing influence is not energetic but entropic in origin, specifically being related to the entropy associated with the mixing of different polyhedra.

Models based on five-fold symmetry were used to describe the structure of  $\text{SiO}_2$  and alkali silicate glasses (e.g., Tilton, 1957). According to this model, the structure is composed of pentagonal dodecahedral cages which cannot be extended indefinitely in three dimensions without accompanying strain of the Si-O bonds. The present author is unaware of applications of five-fold symmetric units to represent the structures of synthetic amorphous polymers, although they have been employed to describe biological macromolecules.

#### Meander Model

According to this model, the structures of amorphous polymers consist of bundles of nearly straight chains which change their directions by the introduction of gauche segments cooperatively arranged in gauche-areas. In this way either honeycomb or meander-like structures can be produced. The latter were suggested as intuitively more probable (Pechhold, 1971). The typical radius of the meander was suggested to be in the range of 50 Å.

### STRUCTURE OF GLASSES

#### Oxide Glasses

Early controversies between proponents of the crystallite and random network models of oxide glass structure were generally decided in favor of the random network model, based largely on the arguments advanced by Warren (1937, 1941). From the width of the main broad diffraction peak for  $\text{SiO}_2$ , e.g., the crystallite size was estimated as 7-8 Å. Since the size of a unit cell of the corresponding crystalline form is about 8 Å, any crystallites would be only a single unit cell in extent and such structures seem at variance with the notion of a crystalline array. Further, in contrast to silica gel, there is no marked small angle scattering from silica glass, at least down to the range of diffraction angles shown in Fig. 1 above. This was taken as indicating that if crystallites of reasonable size are present, there must be a continuous spatial network connecting them which has a density similar to that of the crystallites.

Because of the wide acceptance of the random network model, it came as a great surprise when electron microscope studies of a number of glasses indicated the presence of heterogeneities on a scale of 50-200 Å. The heterogeneities were present in large volume fractions (in the range of 50%), and were seen in both single component and multicomponent glasses, using both replication and direct transmission electron microscopy. Because of the general acceptance of the random

network model, most reviewers "knew" that glasses were random networks; and the reports of such studies appear in publications such as the Pittsburgh Ceramist (Hummel, 1957) and Industrial and Engineering Chemistry (Prebus and Aichner, 1954).

A rationale for the existence of two-phase structures in glasses as manifestations of a process of liquid-liquid immiscibility was soon provided. Particular attention was directed to a model of liquid-liquid phase separation by a continuous mode of transformation known as spinodal decomposition, rather than by the more familiar mode of nucleation and growth. A linearized theory of spinodal decomposition (Cahn, 1965) predicted the occurrence of interconnected microstructures--i.e., microstructures in which both phases are three-dimensionally interconnected. Such structures were observed for compositions near the middle of a number of miscibility gaps; the flood gates were opened; and reports of two-phase or multi-phase structures in glasses began to proliferate. Evidence for miscibility gaps, both stable and metastable, were found in a large number of glass-forming systems; and it is generally recognized today that liquid-liquid phase separation is a widespread phenomenon, the possibility of whose occurrence must be considered when treating the structure and properties of glasses.

The phenomenology of phase separation in oxide glasses has been reviewed by a number of authors (e.g., Uhlmann and Kolbeck, 1976; Vogel, 1977). Microstructures consisting of discrete second-phase particles are generally seen near the boundaries of miscibility gaps (volume fractions of second-phase material less than 15-20%), while interconnected microstructures are often, but not invariably, observed in the central regions of miscibility gaps.

In many glass-forming systems, even more complex phase arrays can be produced as a result of liquid-liquid immiscibility. It has been demonstrated, for example, that a multiplicity of amorphous phases can be produced by appropriate heat treatment of various compositions (Vogel, 1971), and that secondary phase separation is a phenomenon of potential importance in many glasses (e.g., Seward et al., 1968a, and Porai-Koshits and Averjanov, 1968). The latter phenomenon occurs when on cooling a liquid, initial separation takes place into two phases; and on further cooling, one or both of the initial phases in turn separates into other phases, at least for regions away from the inter-phase boundaries.

Caution should be exercised in inferring the mechanism of phase separation from the form of the observed structures. It has been noted, for example, that interconnected microstructures can be produced by the formation, growth and coalescence of discrete second-phase particles, and that discrete-particle structures can be produced by heat treatment of interconnected structures (Seward et al., 1968b).

It has also been noted that inclusion of the leading higher-order nonlinear terms in the theory of spinodal decomposition leads to a breakup of the inter-connectivity seen in the early stage, linear treatment.

Recognizing the occurrence of phase separation, the issue of present concern is the structure of the individual phases in two-phase or multi-phase glasses. To the present author's knowledge, there have been no studies which answer this question unequivocally. The success of the random network model in representing the structure of both single component and single-phase binary glasses suggests, however, that it should usefully describe the structures of the individual phases in phase-separated glasses.

X-ray diffraction studies carried out during the past 10-15 years have established that the random network model provides the best description of the structure of a number of simple glasses, including  $\text{SiO}_2$ ,  $\text{GeO}_2$ , and a number of alkali

silicates. Experimental techniques were developed to eliminate problems associated with Compton scattering and permit reliable data to be obtained out to large values of  $\sin \theta/\lambda$  (here  $\theta$  is the diffraction angle and  $\lambda$  is the wavelength). Compton scattering is of particular concern for materials composed of elements of low atomic number, and hence for many of the important oxide glasses. In the case of  $\text{BaO}_3$ , e.g., at large values of  $\sin \theta/\lambda$ , the incoherent Compton scattering, which contains no structural information, exceeds the coherent scattering by a factor of about four.

In an already-classic paper, Mozzi and Warren (1969) used the technique of fluorescence excitation to eliminate the Compton scattering and determine the structure of glassy  $\text{SiO}_2$ . They found the random network model to provide the best representation of the structure; and they determined that the essential structural randomness of the glass resulted both from a variation in Si-O-Si bond angles, which is notably broader than that of cristobalite, as well as from a distribution of rotation angles of one tetrahedron with respect to an adjacent tetrahedron. In this and subsequent studies of glassy  $\text{SiO}_2$ , no evidence was found for the edge-opposite-face orientations of tetrahedra which are commonly seen in crystalline silicates.

In the case of  $\text{GeO}_3$ , it was found (Uhlmann and Wicks, 1979) that the distribution of Ge-O-Ge angles in the glass is nearly as sharp as that in the crystal. It was suggested that the essential structural randomness of glassy  $\text{GeO}_2$  results from a random distribution of rotation angles of one tetrahedron with respect to an adjacent tetrahedron.

Wicks and Uhlmann also found that the random network model provided the best representation of the structure of a number of single-phase alkali silicate glasses. Some evidence was found, however, for the pairing of alkali ions in the structure. Other evidence for pairing has been provided by other diffraction studies of multicomponent glasses (see the excellent review of this and other aspects of the structure of oxide glasses by Porai-Koshits, 1977).

Other workers have interpreted diffraction data on these glasses using modified crystallite models (e.g., Konnert and Karle, 1973). Strong support for the random network model has, however, been provided by a series of small angle X-ray scattering studies (Weinberg, 1962; Pierre et al., 1972; Renninger and Uhlmann, 1973; Porai-Koshits et al., 1973). For both  $\text{SiO}_2$  and  $\text{GeO}_2$ , an asymptotic small angle intensity is observed, whose magnitude is within a factor of 1.5 of that predicted from thermodynamic fluctuation theory for thermal density fluctuations frozen-in at the glass transition. These findings provide strong evidence against the occurrence of crystallites as the basic structural units of the materials.

An interesting question has arisen concerning whether the thermal density fluctuations are in fact frozen-in at the glass transition, or whether one should anticipate a change in the fluctuation scattering with decreasing temperature below the glass transition. For a number of glassy polymers, Wendorff and Fischer (1973) found in an important study that the asymptotic scattering decreased linearly with falling temperature below the glass transition.

In the case of  $\text{SiO}_2$ , a beautiful investigation of this issue was carried out by Porai-Koshits et al. (1974), who measured the asymptotic small angle X-ray scattering from glassy  $\text{SiO}_2$  over a range from room temperature to 1000°C. It was found that the level of asymptotic scattering was constant over this broad range of temperature, indicating strongly that the thermal density fluctuations are frozen-in at the glass transition. The origin of the difference in behavior between polymer glasses and oxide glasses remains unexplained.

If the wide angle X-ray diffraction studies of  $\text{SiO}_2$  and  $\text{GeO}_2$  glasses indicate random network structures, how is one to explain the electron microscope

observations? This issue was addressed by Seward and Uhlmann (1972) who carried out detailed electron microscope observations of glassy  $\text{SiO}_2$ . It was found that heterogeneities were only sometimes seen, and when seen, depended on the techniques used to prepare samples for the electron microscope observations. It was suggested, therefore, that the original observations of heterogeneities in the single-phase glasses should not be taken as representative of the structure of the materials.

In the case of  $\text{B}_2\text{O}_3$ , the structure does not seem to be composed of a random network of  $\text{BO}_3$  triangles. Rather, a random array of boroxyl units was suggested by Mozzi and Warren (1970), while an array of twisting ribbons of triangles without inter-ribbon correlations was suggested by Funleyev and Cooper (1976).

For all of the oxide glasses studied using modern diffraction and computational techniques, the best representations of the structure are not provided by models based on crystallites, micelles or nodules, paracrystals, or structures having five-fold symmetries. Rather, the best descriptions of the structure seem to be provided by random array models. At least in the case of  $\text{B}_2\text{O}_3$ , the random arrays are of units larger than the basic structural unit of the material ( $\text{BO}_3$  triangles). This may hold as well for other glasses, where the random network may consist of entities larger in scale than the fundamental units of the structure.

#### Polymer Glasses

In the case of glassy thermoplastics, the structural model of a random coil achieved wide acceptance, similar to that accorded to the random network model in the case of oxide glasses. This acceptance was based on a number of findings, which have been summarized by Flory (1972). These include: (1) treatments of models for liquids of chain molecules strongly suggest that states of intermediate order between that of a crystal and a liquid with only short range order have higher free energy than the crystal or liquid; (2) dilution of a bulk polymer changes the elastic modulus gradually, and by only a few percent for dilutions as large as 20%, in contrast to the rapid change with small dilutions expected for initial packing of chains to high density; (3) the close agreement of the mean square chain length of the free chain determined from stress-temperature coefficients of bulk polymer networks with those determined from the intrinsic viscosities (evaluated for infinite dilution) of the same polymers; (4) the close agreement of the mean square chain length of the free chain determined from cyclization equilibria in bulk and in solution, as well as from intrinsic viscosities; and (5) the similarity of thermodynamic interaction parameters evaluated from vapor pressures and from chromatographic measurements.

Direct wide angle X-ray scattering studies of amorphous polymers date back to the well-known investigation of Simard and Warren (1936) of natural rubber. It was indicated by these workers that it was not necessary to make any specific assumptions as to the mutual orientations of the chains in order to describe the X-ray diffraction pattern and derived radial distribution function. A number of subsequent investigators applying wide angle X-ray diffraction techniques to the determination of polymer structures also indicated that no definite conclusion could be made concerning the intermolecular chain packing, while some workers suggested that their data indicated the presence of frequently-occurring and relatively sharp intermolecular distances (and hence some local ordering of the chains).

Consideration of the criticality of diffraction data at large  $\sin \theta/\lambda$  for making precise structural determinations of amorphous materials, the importance of Compton scattering at large  $\sin \theta/\lambda$  (which can exceed the coherent scattering by more than an order of magnitude in case of the hydrocarbon polymers) and the fact that the techniques used in these investigations did not satisfactorily eliminate or

compensate for the Compton scattering, coupled with the notable success of the random coil model in predicting the properties of amorphous polymers and the arguments of Goveas cited above, led to the general neglect of diffraction data concerning intermolecular ordering and general acceptance of the random coil picture.

More recently, closely parallel to those in the field of oxide glasses discussed above, but occurring later in time, electron microscope observations of a large number of glassy thermoplastics indicated the presence of heterogeneities on a scale of several Å. These heterogeneities, termed nodules, were reported to be present in large volume fractions (in the range of 50%), were seen in both stereoregular and atactic polymers, and were observed in both bright field and dark field electron microscopy. The nodular structures were reported to change with volume in the process history of the samples. In particular, they were observed to increase in size and/or rearrange upon annealing and to align upon stretching; in some cases, the nodules were suggested to merge on annealing into patches, which in turn aggregate to form lamellar crystalline structures. These nodular heterogeneities were taken as strong evidence against the random coil model, and strong support for the existence of regions of local order in the materials. (For summaries of the observations of nodules, see Yen (1972) and Uhlmann (1973).)

More recently developments in the field of oxide glasses, subsequent investigations of the structure of amorphous thermoplastics have indicated that the nodular features are not representative of the structure of the bulk polymers; this conclusion is based on direct structural investigations of four types: (1) small angle neutron scattering; (2) small angle X-ray scattering; (3) wide-angle X-ray scattering and (4) light scattering. In addition, investigations of the optical anisotropy of polymers have provided further evidence against the existence of ordered regions as characteristic structural features of glassy polymers.

The small-angle neutron scattering studies have investigated the scattering of deuterated polymers (e.g., polystyrene) in hydrogenated matrices (e.g., elastomer). The deuterated and hydrogenated polymers were synthesized with closely similar molecular weights. The significant finding of these studies was that the radii of gyration of the bulk polymers were found to be the same, *within experimental error*, as those of the polymers in "solvents" (where the random coil model is widely acknowledged as providing a good representation of the chain conformation). Such small-angle neutron studies have been carried out on a series of polystyrenes of different molecular weights (Kignoff et al., 1974) and on polycrylate networks (Kirste et al., 1979).

Small-angle X-ray scattering studies have been carried out on a series of glassy polymers, including polystyrene, polycarbonate, glassy polyethylene terephthalate, poly(methyl methacrylate), and polyvinyl chloride. For all the polymers, an unexpected small-angle scattering intensity was observed whose magnitude was in close agreement with that predicted for thermal density fluctuations frozen-in at the glass transition.

A typical example of these results is shown in Fig. 2 for polycarbonate. Shown in the figure are the measured intensity, the intensity expected for thermal density fluctuations together with a small concentration of heterogeneities (in the range of 0.01%), and the calculated intensity for nodular features present in the reported high volume fraction having crystal excess density. It is seen that the form and magnitude of the scattering expected for the observed nodules in this material is inconsistent with the experimental data. The magnitude of the scattering in the constant-intensity region is  $0.34 \text{ (electrons)}^2 \text{ \AA}^{-3}$ . For comparison, the scattering expected for thermal density fluctuations is about  $0.18 \text{ (electrons)}^2 \text{ \AA}^{-3}$ . Similar results were found for each of the polymers, both

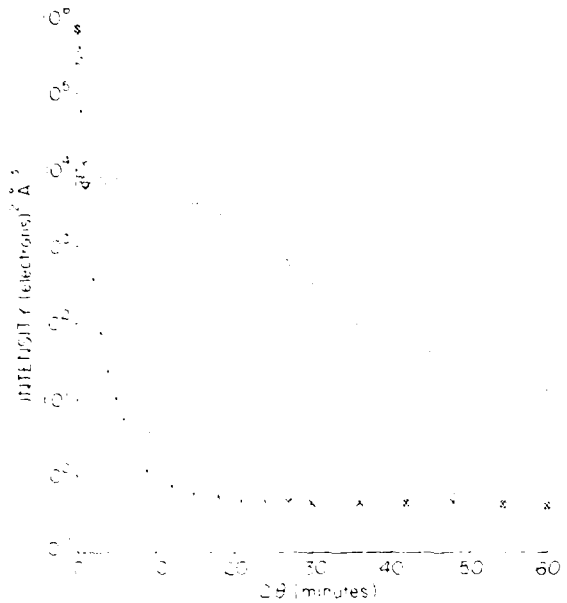


Figure 2  
Absolute SAXS intensity,  $I(\theta)$ , versus scattering angle,  $\theta$ , in minutes. (●), denoted experimental data; (—), calculated intensity for no chain thermal fluctuation,  $\delta v_{\text{ex}} = 0$ ; volume of heterogeneities, 8 nm in diameter and having the crystal excess density; ( $\Delta$ ), calculated intensity for no chain thermal fluctuation, 10 nm in diameter, and having the crystal excess density; ( $\circ$ ), calculated intensity for 20 nm in diameter, and having the crystal excess density. After Schinnerer et al. (1979).

In our laboratory, we are grateful to Dr. J. Fischer and to Professor Fischer's laboratory in Göttingen (Germany) and to Dr. S. H. Glotin.

Modern wide-angle X-ray scattering studies of glassy polymers are illustrated as the work of Winnik and coworkers (Winnik and Leventis, 1980). Using the former study as an example, the radial distribution functions for polycarbonate glasses having different tactic configurations were found to be virtually identical, and only suggestion of correlations attributable to intermolecular ordering was observed. This suggests that little if any intermolecular ordering is associated in either polymer.

In different contexts, it has been proposed that weak effects on the same polycarbonate may be due to the absence of thermally excited excitations to eliminate Raman scattering. No such effect was found, and more or less definite sharp frequency-dependent intermodulation peaks were obtained with glassy structures also giving strong evidence of molecular motion. Evidence of some weakly interacting fractions in the system.

In addition to these studies, attention could be directed to the effects of the temperature on the light scattering. This is important in the determination of the amorphous state. It is often found for an increase in the temperature that the size of clusters in the polymers in the tetrahedral form decreases, which is usually expected for nodular structures, as regions of local order.

and the electron density of the polymer chain. The electron density of the polymer chain is determined by the nature of the substituents on the polymer chain. The electron density of the polymer chain is also determined by the nature of the substituents on the polymer chain.

The electron density of the polymer chain is determined by the nature of the substituents on the polymer chain.



Fig. 3. Electron micrograph of oriented poly(1,3-phenylene terephthalic anhydride) with intrinsic electron density contrast. The electron microscope was operating at 100 kV.

the electron density of the polymer chain. The electron density of the polymer chain is determined by the nature of the substituents on the polymer chain. The electron density of the polymer chain is also determined by the nature of the substituents on the polymer chain.

The electron density of the polymer chain is determined by the nature of the substituents on the polymer chain.

The electron density of the polymer chain is determined by the nature of the substituents on the polymer chain.

thermoplastics should be regarded as random amorphous arrays, with small concentrations of heterogeneities superimposed on thermal density fluctuations frozen-in at the glass transition.

Similar observations of heterogeneities have been made for thermosetting polymers. Heterogeneities, generally on a scale of 50-3000 Å and present in large volume fractions, have been observed in transmission electron microscope studies of a number of cured epoxy resins. Among such studies those of Koutsy and his co-workers (1979, e.g.) and of Morgan and O'Neal (1979, e.g.) have provided the most clear-cut evidence for the presence of structural inhomogeneities. The former workers used replica electron microscopy and observed heterogeneities (which they termed nodular structures) on free surfaces, fracture surfaces and etched surfaces of epoxy resins of widely different cures and chemistries. Further, the heterogeneities were reported to align in the direction of crack propagation (perpendicular to the crack front) on fracture of the epoxy specimens. The sizes of the heterogeneities seen in these studies were generally in the range of 100-300 Å.

Morgan and O'Neal used both replica and direct-transmission electron microscopy as well as scanning electron microscopy to characterize the structural features of epoxy resins. They reported heterogeneities on a number of scales, with particles 60-90 Å in diameter suggested as intramolecularly crosslinked molecular domains which could interconnect to form larger network arrays.

A recent small angle X-ray scattering study of three epoxy resins (Matyi *et al.*, 1980) indicated the presence of heterogeneities, with the largest concentrations in the range about 150 Å in size. If the densities of these heterogeneities differ only slightly from that of the matrix, as expected for epoxy resins, they could be present in large concentrations.

These observations seemed at variance with the original model of network structure (Flory, 1953) which predicted that a polymer network would be homogeneous with crosslinks distributed throughout the material. More recent theoretical studies of network formation (e.g., Solomon, 1967) have suggested that the formation of inhomogeneities should be a frequent if not generally expected occurrence in the synthesis of networks. Regions differing in crosslink density were suggested to be formed in the polymer, with their extent depending on the chemistry of the systems and the polymerization conditions.

Recent work in our laboratory (Di Filippo *et al.*, 1980) has shed new light on the question. Epon 828 epoxy resins were cured with triethylenetetramine (TETA) following two approaches: the first, the samples were mixed and cured at a single elevated temperature; in the second, the samples were mixed and allowed to stand at room temperature prior to curing at the elevated temperature. Transmission electron microscopy of microtomed and stained samples of these epoxies, using the technique of Z contrast, indicate a homogeneous structure for the samples which were not held at room temperature, and a homogeneous microstructure, with heterogeneities on a scale of 100-200 Å, for the samples which were held at room temperature prior to curing.

These results provide striking support for the original suggestion of Flory. The development of heterogeneities seems to be associated, not with general conditions of network formation, but rather with a phase separation process which yields regions with different concentrations of the curing agent at room temperature. On subsequent reheating, these regions do not go back into solution because of the development of some crosslinking during the room temperature hold; and heterogeneous structures are produced during the cure.

As indicated by this discussion, the phenomenon of phase separation, which took the field of oxide glasses by storm in the late 1950's and early 1960's, also has

its analogue in the case of polymers, where it has long been recognized. Before discussing this in detail, it is important to recognize that even simple polymers represent rather complicated solutions. That is, they consist of molecules having different chain lengths (different molecular weights). In addition, most commercial polymers contain modest to significant concentrations of various additives such as heat stabilizers, ultraviolet stabilizers and process aids.

When two different polymers are mixed, homogeneous phases such as occur widely in metallic and oxide systems are seldom formed. In most cases, mixtures of polymers are characterized by immiscibility. The change in entropy on mixing long chain polymer molecules is generally quite small. Since the enthalpy of mixing is generally positive, it is therefore not surprising that most chemically different polymers do not mix.

The standard thermodynamic theory for the mixing of polymers is based on the classical Flory-Huggins theory (see Flory, 1953). More sophisticated theories of polymer solutions (e.g., Flory, 1965) have been developed and applied to the calculation of phase diagrams for polymer mixtures.

When the different polymers are covalently bonded to each other as in block copolymers, the thermodynamics of phase separation required modification. Descriptions of the thermodynamic of such systems have been developed by a number of investigators (e.g., Krause, 1970); and the understanding and control of microstructures in copolymer systems are areas of considerable activity at the present time.

The general incompatibility of different polymers prevents the preparation of useful blends when the phase separation is macroscopic, but polymers having notably improved properties (e.g., impact resistance) can be obtained when the phase separation occurs on microscopic or submicroscopic scale. In the case of block copolymers, the scale and form of the separated structures can be varied by changing the lengths of the blocks and the thermal and chemical histories of the samples.

The morphology of phase-separated polymers often takes the form of spherical particles of one phase embedded in a matrix of a second phase. Other morphologies, specifically cylinders and lamellae, are observed with increasing volume fraction of second-phase material. In addition to changing morphology by changing composition, the morphology of two-phase block copolymers can also be changed by changing the casting solvent as well as by thermal history. The effect of solvents on the morphology can be associated with the solvation power of the solvents for the respective blocks.

The structural features of heterogeneous polymer systems have been summarized by several authors (e.g., Shen and Kawai, 1977). Evidence for interconnected microstructures, such as those often seen in the central regions of miscibility gaps in oxide systems, have been reported in some instances (e.g., Smolders et al., 1971); but these are relatively rare in polymer systems.

#### CRYSTALLIZATION AND GLASS FORMATION

It is recognized by all at this Conference that the occurrence of glasses is a widespread phenomenon in both oxide and polymer systems. It is customary in both these fields of technology to speak of glass-forming and non-glass forming materials, where reference is implicitly made to the ease of cooling liquids in bulk form to produce amorphous solids.

It has been noted, however, that nearly any liquid will form a glass if cooled sufficiently rapidly, and will form a crystalline or partly crystalline body if

cooled sufficiently slowly. On this basis, it was suggested (Uhlmann, 1972a) that the question to be addressed in considering glass formation is not WHETHER a liquid will form a glass but rather HOW FAST must the liquid be cooled in order that detectable crystallinity be avoided.

Among the few cases where the rate of cooling is not significant in the formation of a glass are the atactic polymers, whose lack of stereo-regularity along the chain imposes configurational constraints on their ability to crystallize. While such polymers may form liquid crystalline arrays, particularly when highly oriented, they will not develop three-dimensional crystallinity no matter how slowly they are cooled. For stereoregular polymers, on the other hand, the importance of cooling rate is similar to that for oxides and other materials when considering glass formation.

In estimating the minimum cooling rate required to form a glass of a given material (termed the critical cooling rate), several kinetic treatments have been advanced. The most general of these, based on the treatment of crystallization statistics (Hopper et al., 1974), provides a detailed description of the state of crystallinity in a body, and can describe phenomena such as crystallization on reheating a glass and the effects of nucleating heterogeneities on glass formation (see, e.g., Onorato and Uhlmann, 1976, and Onorato et al., 1980).

By applying the kinetic treatment to a variety of materials, both organic and inorganic, it has been found that glass formation is favored by a large viscosity at the melting point (found for many good oxide glass-formers), a large rate of increase of viscosity with falling temperature below the melting point (found for many good organic glass-formers), large crystal-liquid surface free energies and hence large barriers to crystal-nucleation, the absence of potent nucleating heterogeneities and the requirement for appreciable solute redistribution for crystallization to take place. Derived from these findings are suggestions that glass formation is favored by a large entropy of fusion, by a large value of  $T_g/T_m$  (glass transition temperature/melting point), by formulations which include sizable concentrations of fluxes (e.g.,  $\text{PbO}$ ,  $\text{FeO}$ ) in the case of oxide melts and the relative absence of "crud" in polymer melts, by superheating the liquid prior to cooling, and by formulating the liquid as a "garbage dump" of ingredients in the cases where phase separation can be avoided.

#### VISCOS FLOW BEHAVIOR

Since the formation of glasses depends so critically on the kinetics of crystallization relative to cooling rates, and the kinetics of crystallization in turn depend on the viscosity, it seems useful to compare briefly the viscous flow and crystallization behavior of oxide and polymer liquids.

#### Oxide Liquids

Under most experimental conditions, the viscosity of oxide liquids is Newtonian in character, with the viscosity being independent of stress. In the range of very high stresses, in the range of  $10^9$  dynes/cm<sup>2</sup>, as the glass transition is approached, the viscosity is observed (e.g., Li and Uhlmann, 1970a) to decrease with increasing stress or shear rate (shear thinning behavior).

For small compositional changes near the end-member network oxides (as  $\text{SiO}_2$  and  $\text{GeO}_2$ ), there is a strong effect of composition on the viscosity; and even adventitious impurities such as  $\text{H}_2\text{O}$  can have a significant effect. For complex multicomponent liquids on the other hand, more modest effects of compositional changes are observed; and adventitious impurities generally have only minor effects on viscosity.

With respect to the variation of viscosity with temperature, most oxide liquids show pronounced curvature in the overall log (viscosity) vs.  $1/T$  relations. In most cases, the behavior at high temperatures seems well represented by the free volume model; and a recent development by Grest and Cohen (1979) indicates that a modified free volume model can represent the viscosity over the full range of temperature, although the model has to date been applied primarily to simple liquids.

The only known exceptions for any liquids to the observation of curved log (viscosity) vs.  $1/T$  relations over a wide range of viscosity are the "perfect" tetrahedral network liquids,  $\text{SiO}_2$ ,  $\text{GeO}_2$ , and albite. As shown in Fig. 4, the viscosity-temperature relations for all of these materials indicate Arrhenian behavior over the full range of measured viscosity.

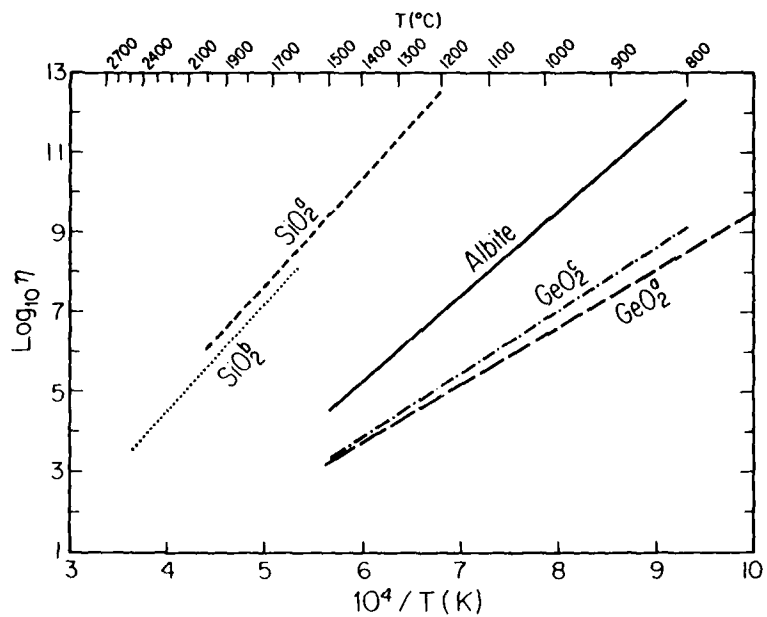


Figure 4  
Variation of viscosity with temperature for  $\text{SiO}_2$ ,  $\text{GeO}_2$ , and albite.  
After Grammer et al. (1980).

Phase separation can have a considerable effect on viscosity. The detailed relationship between viscosity and phase separation is expected to depend on the viscosities of the individual phases, the nature of the diffuse interfaces between the phases, and the size scale and volume fraction of the separated phases. For phase-separating systems, the measured viscosity can be strongly time dependent. For example, the viscosity of a sodium borosilicate glass at a temperature 200° below the immiscibility temperature has been reported to increase by five orders of magnitude over a period of  $10^5$  min. (Simmons et al., 1970). In addition, variations in the kinetics of phase separation with temperature can lead to the unusual result of the viscosity increasing with increasing temperature (Li and Uhlmann, 1970b).

#### Polymer Liquids

The motions involved in the viscous flow of polymers involve segments of the polymer chain. The viscous flow behavior is non-Newtonian in character (shear thinning) at even modest stresses or shear rates, but is Newtonian at sufficiently small shear rates. The usual non-Newtonian behavior is associated with the effects of chain entanglements (e.g., Bueche, 1967); but a fully satisfactory description of these effects remains to be provided.

There is a pronounced effect of the molecular weight on the viscosity of polymer liquids. For polymers of sufficiently high molecular weight, the viscosity in the fluid range increases approximately as  $M^{3.5}$ , where  $M$  is the weight average molecular weight. At temperatures approaching the glass transition, the molecular weight affects the temperature dependence of the viscosity rather than the viscosity itself; and the glass transition temperature is approximately independent of molecular weight above some modest molecular weight.

The temperature dependence of the viscosity at low shear stresses in the fluid range seems well described by a free volume model. The compositional dependence of the viscosity, even near end-member components, is not so dramatic as in the case of oxides. Free volume concepts provide a reasonable description of the effects of composition, although excess entropy treatments have also provided useful insights. The viscosity of both single-component and multicomponent melts is strongly affected by the molecular architecture of the chains (see, e.g., discussion in Bueche, 1967).

When oxide and polymer liquids are compared, the good oxide glass formers are generally characterized by higher viscosities at their melting points than polymer liquids; while crystallizable polymers which readily form glasses usually have a higher rate of increase in viscosity with falling temperature below the melting point.

#### CRYSTALLIZATION BEHAVIOR

##### Oxide Liquids

As first suggested by Jackson (1958), the entropy of fusion is of great importance in considering the crystallization and melting behavior of materials. As noted by Uhlmann (1972b), low entropy of fusion materials ( $CS_M < 2R$ ) have non-faceted interfaces in both crystallization and melting; the crystallization kinetics are largely isotropic; the fraction of preferred growth sites on the crystal-liquid interface is independent of undercooling and superheat; the kinetics are well described by the normal growth model; defects do not significantly affect the kinetics; and the crystallization and melting data are continuous with similar slope through the melting point.

In contrast, high entropy of fusion materials ( $CS_M > 4R$ ) have faceted interfaces in crystallization and non-faceted interfaces in melting; the crystallization kinetics are anisotropic; the fraction of preferred growth sites on the interface increases with increasing undercooling; for most materials, the details of the crystallization kinetics are not well described by any theoretical model, although growth by some form of a surface nucleation mechanism is indicated in many cases; defects are important in growth; and melting is more rapid than crystallization at given small departures from equilibrium.

Of particular note for comparing the crystallization behavior of oxides and polymers, it may be observed that spherulitic growth morphologies are observed in the crystallization of high entropy of fusion materials under conditions of high undercooling and in the presence of impurities. Under conditions where the melt

contains concentrations of impurities in the range of several percent or more, the crystallization kinetics become dominated by diffusional processes, and dendritic growth morphologies are observed.

Also of particular note, the frequency factor for transport at the crystal-liquid interface has been found to scale with the melt viscosity. In detail, the coefficient relating these two quantities is larger than that given by the Stokes-Einstein relation by about a factor of 10. The observed relation between the kinetic coefficient at the interface and the bulk viscosity is consistent with the reconstruction of the structure at the interface involving molecular rearrangements which are similar to those involved in viscous flow (see discussion in Uhlmann, 1972b).

#### Polymer Liquids

The entropy of fusion of polymer liquids is high according to Jackson's criterion (Jackson, 1958). For typical flexible chain polymers, consisting of a distribution of molecular weights, spherulitic growth morphologies are observed under almost all quiescent crystallization conditions. For polymers, as for oxides, there is need for a model to describe spherulitic growth. The treatment which has been most widely used in the polymer field, based on interface instability due to constitutional supercooling, predicts in detail the wrong dimensions of the substructures of the spherulites.

When flexible chain polymers are crystallized under conditions of flow, so-called row nucleated structures are produced. These structures consist of stacked lamellar plates, oriented perpendicular to the direction of flow, which have been likened to shish kebab structures.

The more familiar spherulitic structures consist of radiating arrays of lamellar plates, typically about 100-200 Å in thickness (much smaller than the sizes of the radiating structures in oxide spherulites). These plates are separated by an amorphous phase, which typically occupies about half the volume of the spherulite (also in contrast to oxide spherulites, which generally are completely crystalline).

The lamellar plates in polymer spherulites often branch as they grow. The branching is usually low-angle and non-crystallographic. Twisting of the plates, very likely associated with stresses at their surfaces, is also observed. In addition, there is a central region of the spherulites whose character is different but inadequately characterized (where the original nucleation took place). Finally, there are additives such as stabilizers and process acids, which are found principally in the amorphous regions and inter-spherulite boundaries, and of particular interest at the present time, there are so-called tie molecules which bridge between adjacent crystal plates. Even a simple semicrystalline polymer like polyethylene is thus a rather complicated composite material. For further information on polymer spherulites, see Sharples (1966), Mandelkern (1964) and Uhlmann and Kolbeck (1975).

The polymer molecules in the crystal lamellar are oriented perpendicular to the flat faces of the plates; and since the molecules are usually much longer than the plate thickness, it has been suggested that the molecules fold back and forth during crystallization. The nature of this folding has been suggested by many authors to take place with adjacent re-entry; i.e., the polymer chain re-enters the plate adjacent to where it exited (e.g., Hoffman, 1964).

An alternative view of the structure of the lamellar plates was provided by Flory (1953), who suggested a model for the surfaces of the plates which resembles a telephone switchboard, with little adjacent re-entry, much re-entry to a given plate at positions removed from the exit point, and many interconnections between

lamellae. The differences between these views of the structure of the lamellae plates in melt crystallized flexible chain polymers are shown schematically in Fig. 5.

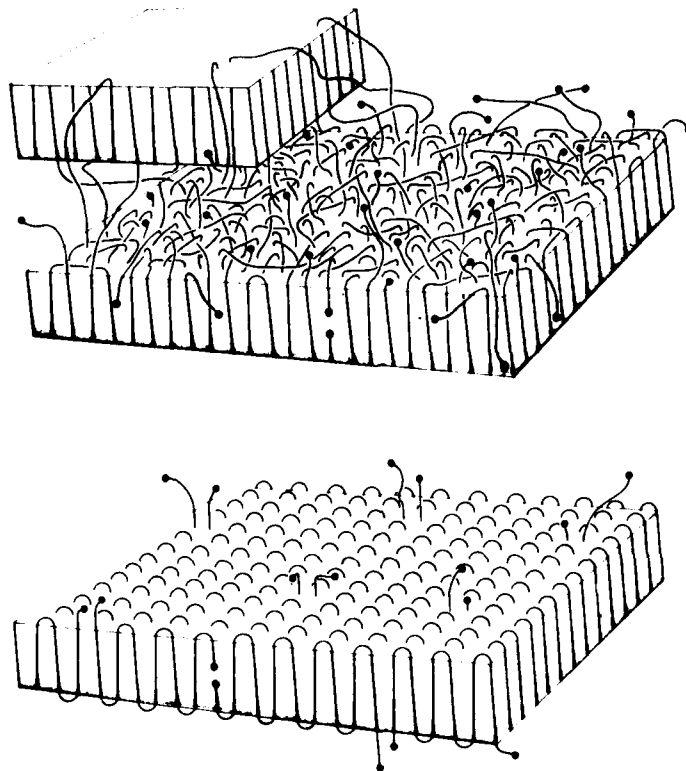


Figure 5  
Schematic illustration of lamellar plates in semi-crystalline polymers. Top figure shows switchboard model; bottom figure shows model of adjacent re-entry folding.

In many parts of the polymer community, the model of adjacent re-entry folding was accepted almost as the word of God revealed to man. This acceptance was based on the basic simplicity of the model and on suggestions such as the surface energies of folded-chain adjacent re-entry configurations are smaller than switchboard configurations. This was deemed noteworthy since the model for growth involved a surface nucleation mechanism with the critical nucleus a single chain segment extending across the crystal face and folding.

Serious objections were, however, raised by some workers to the model of adjacent re-entry folding. The most extensive and wide-ranging series of investigations

in this regard were carried out by Mandelkern and his co-workers (see summary in Mandelkern, 1976). Calvert and Uhlmann (1972) suggested a different model for the growth nucleus, and suggested that "A surface structure resembling a switchboard would then be expected, possibly a switchboard with many of the lines hanging out."

For many workers, however, the results of small angle neutron scattering studies of semi-crystalline polymers such as polyethylene came as a surprise if not a shock. These studies (e.g., Sadler and Keller, 1977; Summerfield et al., 1978; Schelten et al., 1976; Lieser et al., 1975) indicated radii of gyration of the crystallized polymers which are closely similar to those in the melt and in a  $\theta$  solvent. Further, detailed calculations of the scattered intensity by Yoon and Flory (1977, 1980) indicate that the measured scattering is inconsistent with the model of adjacent re-entry folding and indicates an average distance between re-entry points of some 5 or 6 chain diameters.

It was suggested, therefore (Flory and Yoon, 1978), that during the crystallization of a flexible chain polymer from the melt, segments of the chains of about 100-200 Å in length can rearrange into crystalline arrays. The residual amorphous material, which would be highly entangled, is then trapped in the regions between the individual crystalline plates. Such a process would produce a switchboard type of structure with a large number of tie molecules bridging the lamellae plates and with a high degree of chain entanglement in the residual amorphous phase. Similar conclusions were reached by Calvert and Uhlmann (1972) based on calculations of crystallization kinetics and lamellar thicknesses. The conclusion of both these studies, as well as the work of Mandelkern cited above, is that there is insufficient time during crystallization for the chains to disentangle and lay down on the interface as required for adjacent re-entry folding. The scale on which the chain segments can diffuse (rearrange) and form regular arrays is calculated as about 100-200 Å.

Implicit in these calculations is the assumption that transport at the interface can be related to transport in bulk liquid and will scale with the viscosity. As noted in the previous section, this assumption has been amply documented for oxide liquids; and the case for scaling seems even more persuasive for entangled polymer liquids.

To attempt to escape from the implications of the structural view presented above in its kinetic aspects, some proponents of the adjacent re-entry folding model have suggested that the relation between the interface kinetic coefficient and the viscosity does not hold for polymers. Evidence for this has been suggested to be provided by the observation of apparently amorphous polyethylene crystallizing in reasonable times at temperatures below its glass transition (Jones et al., 1979).

It is significant in this regard that the apparently amorphous polyethylene was produced under conditions (casting from solution) where the possibility of retained solvent is real. The situation is similar to that familiar to the oxide glass community. Recall, for example, experience with glassy  $GeO_2$ , whose glass transition temperature is above 500°C but which will develop crystallinity at room temperature in reasonable periods when exposed to a lab atmosphere. The explanation in the latter case seems to be associated with crystallization by a solution-recrystallization process involving water adsorbed from the atmosphere; and a similar process involving solvent is suggested for the results on polyethylene.

Finally, it should be noted that the question of adjacent re-entry folding has not yet been completely resolved. Proponents of such folding now suggest that their model may not be appropriate for the rapidly-quenched polymers examined.

in the small angle neutron scattering studies (the only samples for which such data are available), but that adjacent re-entry folding remains the dominant mode of crystallization under less-rapid solidification conditions.

#### CONCLUDING REMARKS

The formation and structure of polymer and oxide glasses have been considered. It has been noted that the structural characteristics of polymer glasses and oxide glasses have many close similarities. Similarities are also seen in the models used to represent structure, and even in the occurrence of controversies with respect to the existence of ordered regions as representative of the bulk materials. In both types of glasses, the occurrence of phase separation is an important phenomenon to be considered in considering structural features of multi-component systems.

For both types of glasses, controversies concerning structural features seem to be largely resolved; and the structures seem best described by random array models such as the random network or random coil. The random array may, however, consist of structural units larger than the basic units of the material.

The formation of glasses from liquids of either type involves cooling at a sufficient rate that detectable crystallization is not produced. The chain character of polymer melts and the level of chain entanglement in these melts leads to non-Newtonian viscous flow behavior and highly complicated crystallization microstructures. The best model for melt crystallized flexible chain polymers involves lamellar plates, 100-200 Å in thickness, with many molecules bridging adjacent plates, many molecules leaving a given plate and re-entering the plate some distance away, and many chain entanglements in the amorphous phase between the plates; this model remains the source of some controversy at present; as noted by Stockmayer (1974), however, "although nobody can win them all, experienced Flory-watchers are placing their bets."

It is suggested that the kinetic coefficient for transport at the crystal-liquid interface can for typical oxides and polymers be related to the bulk viscosity, and that calculations of crystallization kinetics based on relations between these two quantities can be used in calculating the cooling rates required to form glasses of the respective materials.

Finally, in light of the abundant evidence of similarities in concepts, suggested structures and phenomena for the different classes of materials, it is hoped that the coming decades will see increased interaction between workers in the polymer and oxide glass communities. It is expected that such increased interaction will yield appreciable benefits for both communities.

#### ACKNOWLEDGEMENTS

Financial support for the present work was provided by Air Force Office of Scientific Research and the National Science Foundation. This support is gratefully acknowledged, as are stimulating discussions with Professors P. Flory of Stanford University and D. Turnbull of Harvard University.

*JHM/AF/77-2274*

REFERENCES

- J. D. Bernal (1960) *Scientific American*, August, 1960.
- F. Bueche (1967) *Physical Properties of Polymers*, Wiley, New York.
- J.W. Cahn (1965) *J. Chem. Phys.* 42, 93.
- P.D. Calvert and D.R. Uhlmann (1972) *J. Appl. Phys.* 43, 944.
- M.H. Cohen and G.S. Grest (1979) *Phys. Rev.* 20B, 1077.
- D. Cranmer and D.R. Uhlmann (1980) "Viscosity of Liquid Albite, A Network Material," submitted for publication, *J. Non-Cryst. Solids*.
- G. Di Filippo, J.B. Vander Sande and D.R. Uhlmann (1980) "On the Structure of Glassy Polymers VII. Electron Microscopy of Stained Polymers", submitted for publication, *J. Polymer Sci.*
- F.M. Dunleavy and A.R. Cooper (1976) in Structure of Non-Crystalline Materials.
- P.J. Flory (1953) Principles of Polymer Chemistry, Cornell Univ. Press.
- P.J. Flory (1956) *Proc. Roy. Soc. (Lon.)* A234, 60, 73.
- P.J. Flory (1965) *J. Am. Chem. Soc.* 87, 1833.
- P.J. Flory (1972) *Pure Appl. Chem. Macromol. Chem.* 8, 1.
- P.J. Flory and D.Y. Yoon (1978) *Nature* 272, 226.
- F.C. Frank (1952) *Proc. Roy. Soc.* A215, 43.
- P.H. Geil (1975) *J. Macromol. Sci. (Phys.)* 12, 173.
- E.M. Gyorgy, K. Nassau, M. Eibshutz, J. V. Waszczak, C.A. Wang, and J.L. Shelton (1979) *J. Appl. Phys.* 50, 2883.
- A.C.J. Havermans, H.N. Stein and J.M. Stevens: *J. Non-Cryst. Solids* 5 (1970) 66.
- J.D. Hoffman (1964) *SPE Trans.* 4, 315.
- R.W. Hopper, G.W. Scherer and D.R. Uhlmann (1974) *J. Non-Cryst. Solids* 15, 45.
- R. Hosemann and S. Bagchi (1962) Direct Analysis of Diffraction of Matter, North Holland, Amsterdam.
- F.A. Hummel (1957) *Pittsburgh Ceramist* 9, 1.
- K.A. Jackson (1958) in Growth and Perfection of Crystals, Wiley, New York.
- J. Jones, S. Barenberg and P.H. Geil (1979) *Polymer* 20, 903.
- R.G. Kirste, W.A. Kruse and K. Ibel (1975) *Polymer* 16, 120.
- J.H. Konnert and J. Karle (1973) *Acta Cryst.* 29A, 702.
- S. Krause (1970) *Macromol.* 3, 84.
- J. H. Li and D.R. Uhlmann (1970a) *J. Non-Cryst. Solids* 3, 127.
- J. H. Li and D.R. Uhlmann (1970b) *J. Non-Cryst. Solids* 3, 205.

- G. Lieser, E.W. Fischer and K. Ibel (1975) *J. Polymer Sci.-Polymer Letters* 13, 39.
- R. Lovell, G.R. Mitchell and A.H. Windle (1980) in *Faraday Disc. Chem. Soc.* 68, to be published.
- L. Mandelkern (1964) *Crystallization of Polymers*, McGraw Hill, New York.
- L. Mandelkern (1976) in *Characterization of Materials in Research*, Syracuse Univ. Press, Syracuse.
- R.J. Matyi, D.R. Uhlmann and J.A. Koutschy (1980) *J. Polymer Sci.-Phys.* 18, 1053.
- M. Meyer, J.B. Vander Sande and D.R. Uhlmann (1978) *J. Polymer Sci.-Phys.* 16, 2005.
- J.S. Mijovic and J.A. Koutschy (1979) *J. Appl. Polymer Sci.* 23, 1037.
- K.J. Morgan, J.E. O'Neil and D.B. Miller (1979) *J. Matls. Sci.* 14, 109.
- R.L. Mozzi and B.E. Warren (1969) *J. Appl. Cryst.* 2, 164.
- R.L. Mozzi and B.E. Warren (1970) *J. Appl. Cryst.* 3, 251.
- G. Nielsen and M. Weinberg (1979) *J. Non-Cryst. Solids* 34, 137.
- P.I.K. Onorato and D.R. Uhlmann (1976) *J. Non-Cryst. Solids* 22, 367.
- P.I.K. Onorato, D.R. Uhlmann and R.W. Hopper (1980) "A Kinetic Treatment of Glass Formation. IV. Crystallization on Reheating a Glass," accepted for publication, *J. Non-Cryst. Solids*.
- C. Patterson (1976) *J. Macromol. Sci.-Phys.* B12, 27.
- W. Pechhold (1971) in *Molecular Order-Molecular Motion: Their Response to Macroscopic Stresses*, Wiley, New York.
- A. Pierre, D.R. Uhlmann and F.N. Molea (1972) *J. Appl. Cryst.* 5, 216.
- E.A. Porai-Koshits (1977) *J. Non-Cryst. Solids* 25, 86.
- E.A. Porai-Koshits and V.I. Averjanov (1968) *J. Non-Cryst. Solids* 1, 29.
- E.A. Porai-Koshits, V.V. Golubkov and A.P. Titov (1974) in *Proceedings X Intnl. Congress on Glass*, Kyoto, pp. 12, 1-12, 8.
- A.F. Prebus and J.W. Michener (1954) *Ind. Eng. Chem.* 46, 147.
- A.L. Renninger and D.R. Uhlmann (1974) *J. Non-Cryst. Solids* 16, 325.
- A.L. Renninger, G.G. Wicks and D.R. Uhlmann (1975) *J. Polymer Sci.-Phys.* 13, 1247.
- E.G. Rowlands and P.F. James (1979a) *Phys. Chem. Glasses* 20, 1.
- E.G. Rowlands and P.F. James (1979b) *Phys. Chem. Glasses* 20, 9.
- D.M. Sadler and A. Keller (1977) *Macromolecules* 10, 1128.
- S. Sakka (1980) "Unusual Glasses" in *Frontiers of Glass Science*, to be published.

- J. Schelten, D.G.H. Ballard, G.D. Wignall, G. Longman and W. Schmatz (1976) *Polymer* 17, 751.
- G.W. Scherer and P.G. Schultz (1980): "Unusual Methods of Producing Glass," to appear in *Treatise on Glass*, Vol. 3, Academic Press, New York.
- T.P. Seward and D.R. Uhlmann (1972) in *Amorphous Materials*, Wiley, New York, pp.
- T.P. Seward III, D.R. Uhlmann and D. Turnbull (1968a) *J. Am. Ceram. Soc.* 51, 278.
- T.P. Seward III, D.R. Uhlmann and D. Turnbull (1968b) *J. Am. Ceram. Soc.* 51, 634.
- A. Sharples (1966) *Introduction to Polymer Crystallization*, St. Martin's Press, New York.
- M. Shen and H. Kawai (1978) *Am. Inst. Chem. Engr. J.* 24, 1.
- G.L. Simard and B.E. Warren (1936) 58, 507.
- J.H. Simmons, P.B. Macedo, A. Napolitano and W. Haller (1970) *Disc. Faraday Soc.* 50, 155.
- C.A. Smolders, J.J. van Aartsen and A. Steenbergen (1971) *Kolloid z. u. Z. Polymere* 233, 14.
- D.H. Solomon (1967) *J. Macromol. Sci., Rev. Macromol. Chem.* C1, 179.
- W.H. Stockmayer (1974) *Science* 186, 724.
- G.C. Summerfield, J.S. King and R. Uhlmann (1978) *J. Appl. Cryst.* 11, 548.
- L.W. Tilton (1957) *J. Res. NBS* 59, 139.
- D.R. Uhlmann (1972a) *J. Non-Cryst. Solids* 7, 337.
- D.R. Uhlmann (1972b) in *Advances in Nucleation and Crystallization in Glasses*, American Ceramic Society, Columbus.
- D.R. Uhlmann (1980) in *Faraday Disc. Chem. Soc.* 68, to be published.
- D.R. Uhlmann and A.G. Kolbeck (1975) *Scientific American*, December.
- D.R. Uhlmann and A.G. Kolbeck (1976) *Phys. Chem. Glasses* 17, 146.
- D.R. Uhlmann and G.G. Wieks (1979) *Wiss. Z. Friedrich-Schiller - Univ. Jena, Math. Naturwiss Reihe* 28, 231.
- N.N. Valenkov and E.A. Porai-Koshits (1936): *Z. Krist.* 95, 195.
- W. Vogel (1971) *Structure and Crystallization of Glasses*, Pergamon New York.
- W. Vogel (1977) *J. Non-Cryst. Solids* 25, 170.
- B.E. Warren (1937) *J. Appl. Phys.* 8, 645.
- B.E. Warren (1941) *J. Am. Ceram. Soc.* 24, 256.

- B.E. Warren and J. Biscoe (1938) *J. Am. Ceram. Soc.* 21, 49.
- D.L. Weinberg (1962) *J. Appl. Phys.* 33, 1012.
- J.R. Wendorf and E.W. Fischer (1973) *Kolloid Z. u. Z. Polymere* 251, 876.
- G.G. Wicks (1975) *Structural Studies of Amorphous Materials*, Ph.D. Thesis, MIT.
- G.B. Wignall, D.G.H. Ballard and J. Schelten (1974) *Europ. Polymer J.* 10, 861.
- G.B. Wignall and G.W. Longman (1973) *J. Matls. Sci.* 8, 1439.
- G.S.Y. Yeh (1972) *Crit. Rev. Macromol. Chem.* 1, 173.
- D.Y. Yoon and P.J. Flory (1977) *Polymer* 18, 509.
- D.Y. Yoon and P.J. Flory (1980) in *Faraday Disc. Chem. Soc.* 68, to be published.
- K.H. Zachariasen (1932) *J. Am. Chem. Soc.* 54, 3841.
- J. Zarzycki and R. Mezard (1962) *Phys. Chem. Glasses* 3, 163.

## Structure of Glassy Polymers. VII. Small-Angle X-Ray Scattering from Epoxy Resins\*

R. J. MATYI<sup>†</sup> and D. R. UHLMANN, *Department of Materials Science and Engineering, Massachusetts Institute of Technology, Cambridge, Massachusetts 02139* and J. A. KOUTSKY, *Department of Chemical Engineering, University of Wisconsin, Madison, Wisconsin 53706*

### Synopsis

The small-angle x-ray scattering (SAXS) from an Epon 812 and two Epon 828 (one amine-cured and one anhydride-cured) epoxy resins has been measured using a Bonse-Hart system. The data cover the angular range ( $2\theta$ ) between 20 sec and 60 min. After correction for absorption, background and vertical beam divergence, they have been placed on an absolute basis by comparison with the scattering from a previously studied polycarbonate sample. The corrected absolute intensity decreases strongly with increasing angle between 20 sec and 2 min, decreases more gradually between 2 and 20–30 min, and reaches a nearly constant asymptotic value at larger angles. The magnitude of the intensity in the constant-intensity region is close to the value predicted by thermodynamic fluctuation theory for fluids applied at the glass transition temperature. The increase in intensity at angles smaller than 20–30 min is associated with heterogeneities in the cured resins. These heterogeneities cover a range of sizes in all samples, from less than 100 Å to more than 1000 Å, with the most frequently occurring size in the range 100–200 Å.

### INTRODUCTION

The structures of five glassy thermoplastics—polycarbonate, poly(methyl methacrylate), poly(ethylene terephthalate), poly(vinyl chloride), and polystyrene—have so far been examined using small-angle x-ray scattering (SAXS). In each case,<sup>1–5</sup> the measured intensity at scattering angles ( $2\theta$ ) greater than 10–40 min approaches or reaches the asymptotic value expected for thermal density fluctuations frozen-in at the glass transition. At smaller angles, the intensity increases strongly with decreasing angle. The increased scattering at very small angles was associated with small concentrations of large (several hundred to several thousand Å diameter) heterogeneities. These heterogeneities were suggested to be extrinsic to the polymer (air bubbles, dirt, process aids, etc.).

The data obtained in these studies are at variance with previous claims of nodular structures in the polymers. Specifically, the measured intensity is inconsistent, both in magnitude and in its variation with scattering angle, with the presence of nodules as representative of the bulk material. Subsequent electron microscopy studies on four of the glassy thermoplastics have yielded results consistent with the SAXS data and indicate the general absence of microstructural features down to sizes approaching the resolution limit of the electron microscope.

\* Based in part on a thesis submitted by R.J.M. in partial fulfillment of the requirements for the M.S. degree in Materials Science, MIT, 1976.

<sup>†</sup> Now with Northern Petrochemical Co., Morris, IL.

While most of the controversy surrounding the existence of nodules has centered about thermoplastic polymers, many studies have been conducted on network-forming thermosetting polymers as well. The original simple model of network structure<sup>6</sup> predicted that a polymer network would be homogeneous with crosslinks distributed throughout the material at random. More recent theoretical studies of network formation (see e.g., refs. 7-9), employing more sophisticated mathematical treatments, have shown that the formation of inhomogeneities should be a frequent if not generally expected occurrence in the synthesis of networks. In many systems, the chemical reactions are diffusion controlled and are not carried through to completion; and heterogeneous structures can be produced. More generally, regions differing in crosslink density can be formed in the polymer, their extent depending on the chemistry of the system and the polymerization conditions.

Heterogeneities, generally on a scale of 50-3000 Å and present in large volume fractions, have been observed in transmission electron microscope studies of a number of cured epoxy resins (see e.g., refs. 10-16). Among such studies, those of Koutsky and his co-workers<sup>12,13</sup> and of Morgan and O'Neal<sup>14-16</sup> have provided the most clear-cut evidence for the presence of structural inhomogeneities. The former workers used replica electron microscopy and observed heterogeneities (which they termed nodular structures) on free surfaces, fracture surfaces and etched surfaces of epoxy resins of widely different cures and chemistries. Further, the heterogeneities were reported to align in the direction of crack propagation (perpendicular to the crack front) on fracture of the epoxy specimens. The sizes of the heterogeneities seen in these studies were generally in the range of 100-300 Å.

Morgan and O'Neal<sup>14-16</sup> used both replica and direct-transmission electron microscopy as well as scanning electron microscopy to characterize the structural features of epoxy resins. They reported heterogeneities on a number of scales, with particles 60-90 Å in diameter suggested as intramolecularly crosslinked molecular domains which could interconnect to form larger network arrays.

Because of the similarity of these observations to those reported previously for thermoplastic polymers, the widespread nature of reported heterogeneities in cured epoxy resins, and the potential importance of such heterogeneities for affecting the properties of the resins, it was decided to undertake an examination of crosslinked epoxy resins using SAXS. The epoxy resins were crosslinked with both amine and acid anhydride curing agents.

## EXPERIMENTAL PROCEDURE

Three cured epoxy resin systems were examined in this study. Two of the systems were based on the diglycidyl ether of bisphenol-A (Epon 828, Shell Chemical Co.); the samples were cured with triethylenetetraamine (TETA) and nadic methyl anhydride (NMA). The Epon 828/NMA system was catalyzed by the addition of 1% benzyl dimethylamine (BDMA). The third system was based on the triglycidyl ether of glycerol (Epon 812, Shell Chemical Co.) and was cured with dodecetyl succinic anhydride (DDSA), NMA, and BDMA. The details of the curing agent concentrations, cure times, and cure temperatures are shown in Table I. The Epon 828 samples were mixed by hand for 5 min and vacuum degassed for 10 min before curing in a preheated air oven using the

TABLE I  
Composition and Cure of Sample Systems

Epoxy resin	Cure agent	Concentration (phr) <sup>a</sup>	Time and temperature
Epon 828	TETA	12.0	45 min at 25°C 4 days at 100°C
	NMA	93.9	3 hr at 125°C
Epon 812	DDSA	6.9	14 days at 175°C
	NMA	74	3 hr at 70°C
	DDSA	24	24 hr at 130°C
	BDMA	2	

<sup>a</sup> Parts per hundred of resin by weight.

temperatures and times given in Table I. The Epon 812 sample was mixed by hand for ten minutes, poured into silicone molds, and allowed to stand for twenty minutes to eliminate large bubbles. They were then cured as indicated in Table I. This procedure is identical to that used in preparing the Epon 812 samples in which nodular structures were seen in the electron microscope.<sup>12</sup>

Thin (ca. 0.25 cm) sections were cut from the cured samples and were polished with alumina powder for SAXS examination. The SAXS data were collected using a Bonse-Hart small-angle x-ray scattering system (Advanced Metals Research, Burlington, Mass.). The system was used with CuK<sub>α</sub> radiation and employed pulse height analysis of the output of a scintillation detector. The diffraction geometry, described in detail in ref. 1, permits reliable data to be obtained at scattering angles as small as 10–20 sec.

The data were taken at 10 sec intervals over the range 20 sec  $\leq 2\theta \leq$  1 min, 60 sec intervals over the range 1  $\leq 2\theta \leq$  6 min, 3 min intervals over the range 6  $\leq 2\theta \leq$  30 min, and 6 min intervals over the range 30  $\leq 2\theta \leq$  60 min. For 2θ  $\leq$  6 min, the sample scattering and the background scattering were measured in succession at each angle. For 2θ > 6 min, a master background curve was constructed after several counts had been made at each value of 2θ. Selected background counts performed during each run were used to scale the master curve for values of 2θ > 6 min. A scan of the main beam from –20 to +20 sec was conducted before each run to identify any variations in tube intensity.

Prior to each run, the sample absorption  $e^{-ut}$  (where  $t$  is the sample thickness) was determined by measuring the main beam intensity with the sample in place and then counting the beam with the sample removed. For all samples,  $e^{-ut}$  was between 0.32 and 0.43. The scattered intensity  $\tilde{I}$  at an angle 2θ was then corrected for background and absorption using the relation

$$\tilde{I} = (\tilde{I}_s - N)/e^{-ut} + N - \tilde{I}_b \quad (1)$$

where  $\tilde{I}_s$  is the scattered intensity at an angle 2θ with the sample in place,  $\tilde{I}_b$  is the background intensity at the same angle, and  $N$  is the system noise level.

The experimental intensities were corrected for slit smearing effects by the method described by Renninger et al.<sup>1</sup> This desmearing procedure, based on an iterative deconvolution process, is valid if the sample is isotropic and if the horizontal divergence of the beam is negligible compared to the vertical divergence. Both assumptions are warranted in the present study due to the nature of the material (epoxy resins cast in bulk) and the geometry of the Bonse-Hart system (see discussion in ref. 1).

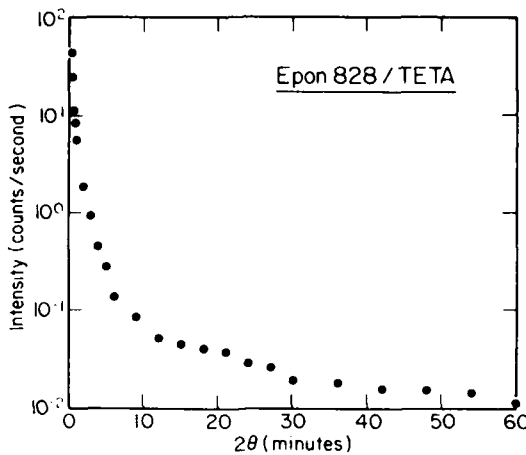


Fig. 1. Experimental SAXS intensity from Epon 828/TETA.

The desmeared data were put on an absolute basis through a comparison with the desmeared scattering curve obtained from a well-characterized sample of polycarbonate, (Lexan, General Electric Co.), for which absolute intensity data were available.<sup>1</sup> The desmeared polycarbonate curve obtained in this study was in excellent agreement with that obtained previously<sup>1</sup> except for a constant multiplicative factor  $R_{PC}$ . The SAXS data were thus normalized and placed on an absolute basis with the relation

$$R_{\text{sam}} = R_{PC} t_{\text{sam}} / t_{PC} \quad (2)$$

where  $R_{\text{sam}}$  is the sample normalization factor, and  $t_{PC}$  and  $t_{\text{sam}}$  are the thickness of the polycarbonate and epoxy samples, respectively.

## RESULTS AND DISCUSSION

Figures 1-3 show the observed variations of intensity with scattering angle

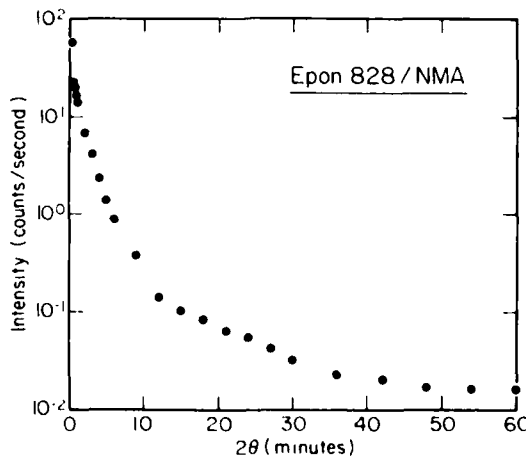


Fig. 2. Experimental SAXS intensity from Epon 828/NMA.

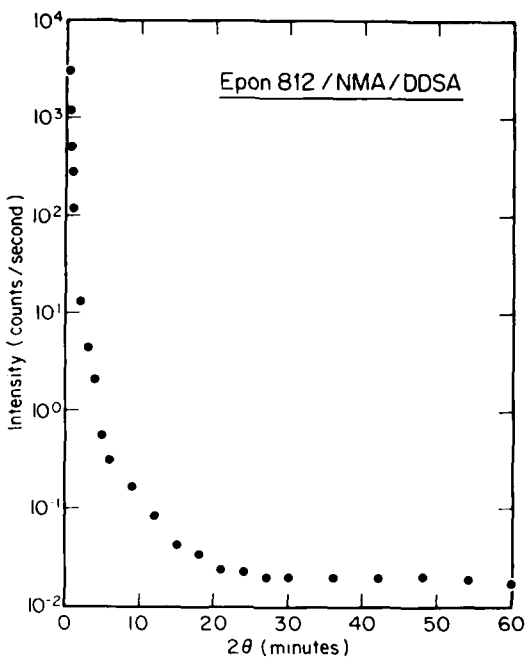


Fig. 3. Experimental SAXS intensity from Epon 812/NMA/DDSA.

for the Epon 828/TETA, Epon 828/NMA, and Epon 812/NMA/DDSA systems, respectively. The desmeared absolute intensity SAXS curves obtained from the three epoxy resin systems are shown in Figures 4-6.

The desmeared scattering curves for the three epoxy systems are qualitatively similar to those obtained from other amorphous polymers. In the angular range  $20 \text{ sec} < 2\theta < 2 \text{ min}$ , the epoxies all display a sharp decrease in scattered intensity. The intensity continues to decrease, but more slowly, as the scattering angle is increased beyond 2 min. Both of the Epon 828 samples show a pronounced

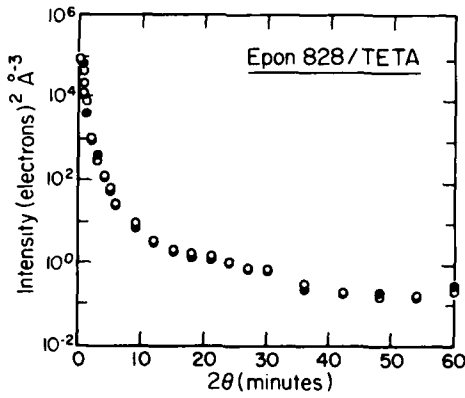


Fig. 4. Variation of absolute SAXS intensity with scattering angle for Epon 828/TETA. (●) Desmeared experimental data; (○) calculated intensity for thermal density fluctuations + distribution of heterogeneities shown in Table II.

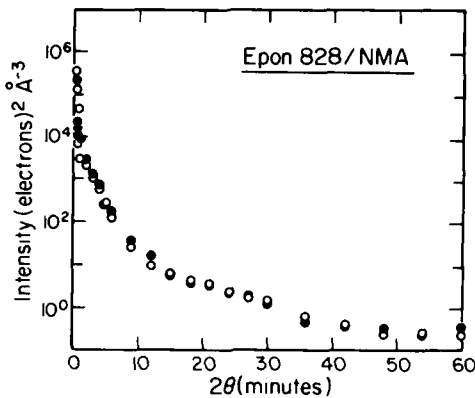


Fig. 5. Variation of absolute SAXS intensity with scattering angle for Epon 828/NMA. (●) Desmeared experimental data; (○) calculated intensity for thermal density fluctuations + distribution of heterogeneities shown in Table III.

leveling of the scattering curve between 15 and 30 min before decreasing to constant levels at relatively large angles ( $2\theta > 40$  min). The Epon 812/NMA/DDSA system displays a smooth decrease in intensity out to approximately 24 min. Beyond that angle, the intensity remains almost constant.

A nearly constant (asymptotic) SAXS intensity at small diffraction angles is expected for an ideal liquid or glass because of the presence of thermal fluctuations in density or composition. The expected magnitude of this scattering may be obtained from thermodynamic fluctuation theory (e.g., ref. 17) and the standard treatment of small-angle x-ray scattering<sup>18</sup>:

$$I(0) = V \langle (\Delta\rho)^2 \rangle = k T K_T \rho^2 \quad (3)$$

where  $K_T$  is the isothermal compressibility,  $\rho$  is the average electron density,  $\langle (\Delta\rho)^2 \rangle$  is the mean square density fluctuation in a region of volume  $V$ , and  $I(0)$  is the zero-angle scattering.

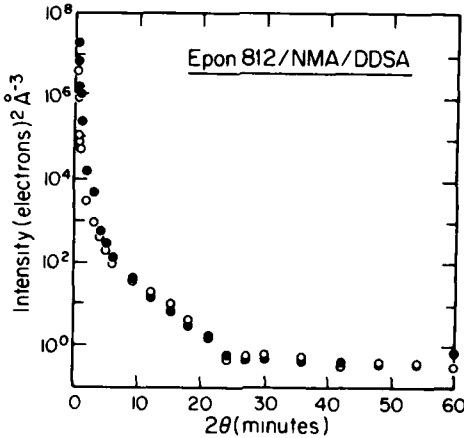


Fig. 6. Variation of absolute SAXS intensity with scattering angle for Epon 812/NMA/DDSA. (●) Desmeared experimental data; (○) calculated intensity for thermal density fluctuations + distribution of heterogeneities shown in Table IV.

Weinberg<sup>19,20</sup> suggested that a glass should retain the configurational (but not the vibrational) fluctuations present in the liquid at the glass-transition temperature  $T_g$ . The expected zero-angle scattering may be written

$$I(0) = k T_g K_T(T_g) \rho^2 \quad (4)$$

Wendorff and Fischer<sup>21</sup> reported that the zero-angle scattering for poly(methyl methacrylate), polycarbonate, and poly(ethylene terephthalate) increases linearly with temperature below the glass transition, and increases linearly as well (but with a higher slope) at temperatures above the glass transition. Rathje and Ruland<sup>22</sup> also reported the zero-angle scattering from poly(methyl methacrylate) and polystyrene increases with temperature below the glass transition; but these workers found a less-sharp transition in slope at  $T_g$ . In contrast, Porai-Koshits<sup>23</sup> and we have found the zero-angle scattering from  $\text{SiO}_2$  to be independent of temperature below the glass transition; and in this case, the scattering data were obtained over a temperature range of more than  $900^\circ\text{C}$  ( $T_g \approx 1000^\circ\text{C}$  for this material). Because of the uncertainty in the expected zero-angle scattering at temperatures below  $T_g$ , eq. (4) will be used to eliminate  $I(0)$ . Because of the limited range of temperature between  $T_g$  and ambient, this expression should in any case be good to within about 25%.

The use of eq. (4) requires a knowledge of both  $T_g$  and  $K_T$  at  $T_g$ . The compressibilities of epoxy resins at elevated temperature are not well documented, however; and it was considered best to measure  $K_T$  experimentally. Castings of the Epon 828 samples were prepared containing strain gauges and were pressurized to 2 kbar at ambient temperature in a hydrostatic pressure vessel. The compressibilities of the samples were determined from the slopes of the compression-strain curves, and these values were used for  $K_T(T_g)$  in eq. (4). It is recognized that this represents an underestimate of the compressibility at  $T_g$ ; but the difference is expected to be modest. The method for determining  $K_T$  could not be employed for the Epon 812/NMA/DDSA systems, however, because the sample was received in the as-cured state and thus could not be tested in the pressure vessel. As an approximation,  $K_T$  of the Epon 812 sample was taken as the average of the Epon 828 compressibilities. The glass transition temperatures of the three samples were determined by differential scanning calorimetry using a Perkin-Elmer DSC-2 apparatus, and the results were used with the compressibility data to evaluate the expected zero-angle scattering.

For the Epon 828/TETA sample, for instance, we have  $\rho = 0.39$  electrons  $\text{\AA}^{-3}$ ,  $K_T = 1.9 \times 10^{-11}$  dyn cm $^{-2}$ , and  $T_g = 105^\circ\text{C}$ . Using these values, we obtain  $I(0) = 0.16$  electrons $^2\text{\AA}^{-3}$ . For Epon 828/NMA, parameters are  $\rho = 0.39$  electrons  $\text{\AA}^{-3}$ ,  $T = 165^\circ\text{C}$ , and  $K_T = 2.2 \times 10^{-11}$  dyn cm $^{-2}$ . Substitution yields  $I(0) = 0.20$  electrons $^2\text{\AA}^{-3}$  for this system. These calculated values compare favorably with the observed asymptotic intensities of 0.18 electrons $^2\text{\AA}^{-3}$  (Epon 828/TETA) and 0.25 electrons $^2\text{\AA}^{-3}$  (Epon 828/NMA). For the Epon 812/NMA/DDSA system, parameters are  $\rho = 0.40$  electrons  $\text{\AA}^{-3}$ ,  $T_g = 130^\circ\text{C}$  and  $K_T$  was assumed to be  $2 \times 10^{-11}$  dyn cm $^{-2}$ . The corresponding expected value of  $I(0)$  is 0.18 electrons $^2\text{\AA}^{-3}$ . This compares with the observed asymptotic intensity of approximately 0.3 electrons $^2\text{\AA}^{-3}$ . DDSA is known<sup>24</sup> to impart flexibility to epoxy castings due to its long aliphatic chains; as a result, the compressibility of the Epon 812/NMA/DDSA material is probably higher than the value used here. Consequently, the calculated value of  $I(0)$  is likely an underestimate of the true

value. The increase in compressibility with increasing temperature would also give rise to larger expected values of the asymptotic scattering.

The pronounced rise in scattered intensity at small angles ( $2\theta < 30$  min) and the excess asymptotic scattering at larger angles (over that predicted by fluctuation theory) can be associated with heterogeneities in the samples. The scattered intensity from spherical particles of radius  $R$  may be expressed as

$$I'(h) = C(1 - c)V(\Delta\rho)^2 \left( 3 \frac{\sin(hR) - hR \cos(hR)}{h^3 R^3} \right) \quad (5)$$

Here  $I'(h)$  is the intensity in excess of the scattering from thermal density fluctuations; and  $h = 4\pi \sin\theta/\lambda$ , where  $\lambda$  is the wavelength of the radiation.

The sizes and concentrations of heterogeneities needed to describe the observed scattering curves for the three samples are shown in Tables II to IV. The presence of large heterogeneities ( $R > 250$  Å) is required to explain the large increase in intensity at very small angles. It is possible that these heterogeneities

TABLE II  
Calculated Sizes and Concentrations of Heterogeneities in Epon 828/TETA ( $\rho = 0.39$   
electrons Å<sup>-3</sup>)

$R$ (Å)	$c(1 - c)(\Delta\rho)^2$	$c(\Delta\rho = 1\%)$	$c(\Delta\rho = 10\%)$ ( $\times 10^{-4}$ )	$c(\Delta\rho = 100\%)$ ( $\times 10^{-6}$ )
75	$1.24 \times 10^{-6}$	0.0895	8.15	8.5
250	$3.46 \times 10^{-7}$	0.0232	2.27	2.27
500	$5.20 \times 10^{-7}$	0.0355	3.42	3.42
1500	$1.11 \times 10^{-6}$	0.0793	7.30	7.30
4000	$4.77 \times 10^{-7}$	0.0325	3.14	3.14

TABLE III  
Calculated Sizes and Concentrations of Heterogeneities in Epon 828/NMA ( $\rho = 0.39$   
electrons Å<sup>-3</sup>)

$R$ (Å)	$c(1 - c)(\Delta\rho)^2$	$c(\Delta\rho = 1\%)$	$c(\Delta\rho = 10\%)$	$c(\Delta\rho = 100\%)$
75	$3.11 \times 10^{-6}$	0.300	$2.10 \times 10^{-3}$	$2.10 \times 10^{-5}$
250	$9.17 \times 10^{-7}$	0.0663	$6.19 \times 10^{-4}$	$6.19 \times 10^{-6}$
500	$3.92 \times 10^{-6}$	...	$2.64 \times 10^{-3}$	$2.64 \times 10^{-5}$
1000	$2.39 \times 10^{-7}$	0.0164	$1.61 \times 10^{-4}$	$1.61 \times 10^{-6}$
4000	$1.86 \times 10^{-6}$	0.147	$1.25 \times 10^{-3}$	$1.25 \times 10^{-5}$

\* Gives  $c(1 - c) > 0.25$ .

TABLE IV  
Calculated Sizes and Concentrations of Heterogeneities in Epon 812/NMA/DDSA ( $\rho = 0.40$   
electrons Å<sup>-3</sup>)

$R$ (Å)	$c(1 - c)(\Delta\rho)^2$ ( $\times 10^{-6}$ )	$c(\Delta\rho = 1\%)$	$c(\Delta\rho = 10\%)$ ( $\times 10^{-3}$ )	$c(\Delta\rho = 100\%)$ ( $\times 10^{-5}$ )
150	3.18	0.266	1.95	1.95
500	1.91	0.135	1.17	1.17
3000	1.77	0.124	1.08	1.08
5000	9.55	...	5.88	5.88
6000	5.53	...	3.38	3.38

\* Gives  $c(1 - c) > 0.25$ .

may be extrinsic to the polymers. While adventitious impurities such as dirt may be responsible for some of this scattering, a more likely source is gas (air) bubbles incorporated in the resin during curing. As seen in Tables II to IV, concentrations of gas bubbles in the range of  $10^{-5}$  are sufficient to account for the observed scattering (above fluctuation scattering) in the very low-angle region. Alternatively, the heterogeneities in this range of large sizes may be supermolecular arrays of regions which differ in crosslink density.

The scattering at larger angles (still in the small-angle region) is associated with smaller heterogeneities. The slow decrease in scattering from the Epon 828 samples in the angular range between 20 and 30 min, and the excess scattering at larger angles (above that due to thermal fluctuations) in all samples, particularly the Epon 812 sample, indicate the presence of small ( $<100 \text{ \AA}$ ) inhomogeneities in the materials. Again, concentrations of gas bubbles in the range of  $10^{-5}$  would be sufficient to account for the observed excess scattering, although the presence of other structural inhomogeneities could also account for the scattering. If the densities of these heterogeneities differ only slightly from that of the matrix (as  $\Delta\rho/\rho = 1\%$ ), they could be present in sizable concentrations (see Tables II-IV).

Figures 4-6 show a comparison of the experimental data with the scattering expected for the distributions of heterogeneities shown in Tables II to IV superimposed on thermal density fluctuations. The indicated distributions of heterogeneities are seen to provide a close description of the data. It should be noted, however, that these distributions are not unique. They simply indicate the ranges of sizes which are needed to describe the experimental data. Any distribution used to describe the scattering must have large particles (in the range of several thousand angstroms) as well as smaller particles (in the range below  $200 \text{ \AA}$ ) in concentrations not greatly different from those indicated in Tables II to IV.

The present results seem at variance with many reported observations of nodular features in cured epoxies as representative of the bulk structure. For studies carried out using direct transmission electron microscopy on thin sections, rather than electron microscopy of replicas, a density difference of about  $0.1 \text{ g cm}^{-3}$  is required to produce observable contrast in a  $1000\text{-\AA}$ -thick sample irradiated with 100 kV electrons.<sup>25</sup> This indicates that inhomogeneities in a  $1000 \text{ \AA}$  thick sample of epoxy would provide discernible contrast only if they differed in density from the bulk by about 5-10%, a difference which is much larger than the change in density on curing. Further, the density difference required for observable contrast increases as the sample thickness decreases. Examination of Tables II to IV shows, however, that heterogeneities differing from the bulk density by 10% or more can only be present at concentrations in the range about 0.1%—a range which is much smaller than the concentrations indicated for the nodular features.

For studies carried out using electron microscopy of surface replicas, which represent the largest fraction of the observations of nodular features in epoxies, a somewhat different question is posed by the present results. The indicated volume fractions of heterogeneities seen in the electron microscopy studies are consistent with the SAXS results only if they differ in density by perhaps 1% or less from the bulk. Considering the small change in density on curing epoxy systems—typically 1% or less—as well as the nature of the curing process, the

occurrence of regions differing in density by only a small amount seems reasonable. It remains to be established, however, how regions with such differences in density become visible on fracture surfaces. Certainly there is good reason for expecting regions of different crosslink density in cured epoxies; and such differences should be reflected in details of the fracture process. What remains to be clarified is the relation between such regions and the features seen in electron microscope studies. The present SAXS results should be viewed as providing data with which any proposed structural model must be consistent.

The sizes of the heterogeneities inferred from the present SAXS data, with largest concentrations in the range about 150 Å, are similar to those reported in several electron microscope studies. Because of concerns about contrast in direct transmission electron microscope studies of epoxies and about the relation between structural features and features seen in electron microscopy of replica surfaces, as well as the differences in chemistry and thermal histories of the epoxies examined, the similarity of sizes will simply be noted here.

### CONCLUSIONS

The small-angle x-ray scattering from three cured epoxy resins—an Epon 812 material, an amine-cured Epon 828, and an anhydride-cured Epon 828—varies with scattering angle in a manner generally similar to that observed previously for glassy thermoplastics. The SAXS intensity from the epoxy samples decreases sharply with increasing angle in the very small angle region ( $2\theta < 2$  min), then less slowly with further increases in angle (out to  $2\theta$  equal to 20 or 30 min) and then approaches a constant asymptotic intensity. As with the glassy thermoplastics, the measured SAXS in the constant-intensity region corresponds closely with that expected for thermal density fluctuations frozen-in at the glass transition. In detail, however, the measured intensity is somewhat higher than that expected for thermal fluctuations, particularly for the Epon 812 sample.

The increase in SAXS intensity at very small scattering angles has been associated with a small concentration of large heterogeneities (exceeding 1000 Å in size). These may well be heterogeneities extrinsic to the polymer, such as gas bubbles introduced during curing of the resins. The presence of small heterogeneities (less than 200 Å in size) is also indicated by the SAXS data. If intrinsic to the polymers, they can be present in large concentrations (tens of percent) if they differ slightly in density from the bulk ( $\Delta\rho/\rho \approx 1\%$ ).

The present results are inconsistent with the presence of nodular structures visible in direct transmission electron microscopy of thin specimens, and set constraints on the characteristics of heterogeneities seen using replica electron microscopy. The precise origin of these heterogeneities is not clear at present. They may be related to regions differing in crosslink density, but the nature of this relation remains to be elucidated satisfactorily.

Appreciation is due to Dr. L. H. Peebles, Jr. of Office of Naval Research for stimulating discussions. Financial support for the MIT portion of the present work was provided by the Air Force Office of Scientific Research. This support is gratefully acknowledged.

AFCR-77-3226

## References

1. A. L. Renninger, G. G. Wicks, and D. R. Uhlmann, *J. Polym. Sci. Polym. Phys. Ed.*, **13**, 1247 (1975).
2. A. L. Renninger and D. R. Uhlmann, *J. Polym. Sci. Polym. Phys. Ed.*, **13**, 1481 (1975).
3. A. L. Renninger and D. R. Uhlmann, *J. Polym. Sci. Polym. Phys. Ed.*, **14**, 415 (1976).
4. R. S. Straff and D. R. Uhlmann, *J. Polym. Sci. Polym. Phys. Ed.*, **14**, 353 (1976).
5. A. L. Renninger and D. R. Uhlmann, *J. Polym. Sci. Polym. Phys. Ed.*, **16**, 2237 (1978).
6. P. J. Flory, *Principles of Polymer Chemistry*, Cornell U. P., Ithaca, NY, 1953.
7. S. S. Labana, S. Newman, and A. J. Chomppf, in *Polymer Networks, Structure and Bulk Properties*, S. S. Labana, S. Newman, and A. J. Chomppf, Eds., Plenum, New York, 1971.
8. K. Dusek, *Collect. Czech. Chem. Commun.*, **33**, 1100 (1968).
9. D. H. Solomon, *J. Macromol. Sci. Rev. Macromol. Chem.*, **C1**, 179 (1967).
10. R. M. Kessenikh, L. A. Korshunova, and A. V. Petrov, *Sov. Phys. J.*, **2**, 126 (1972).
11. J. L. Kardos, *Trans. N.Y. Acad. Sci.*, **II**, **35**, 136 (1973).
12. J. L. Racich and J. A. Koutsky, *J. Appl. Polym. Sci.*, **20**, 2111 (1976).
13. J. S. Mijovic and J. A. Koutsky, *J. Appl. Polym. Sci.*, **23**, 1037 (1979).
14. R. J. Morgan and J. E. O'Neal, *J. Mater. Sci.*, **12**, 1966 (1977).
15. R. J. Morgan and J. E. O'Neal, *Polym. Plast. Technol. Eng.*, **10**, 49 (1978).
16. R. J. Morgan, J. E. O'Neal, and D. B. Miller, *J. Mater. Sci.*, **14**, 109 (1979).
17. H. B. Callen, *Thermodynamics*, Wiley, New York, 1960.
18. A. Guinier and G. Fournet, *Small-Angle Scattering of X-Rays*, Wiley, New York, 1955.
19. D. L. Weinberg, *Phys. Lett.*, **7**, 324 (1963).
20. D. L. Weinberg, *J. Appl. Phys.*, **33**, 1012 (1962).
21. J. H. Wendorff and E. W. Fischer, *Kolloid Z. Z. Polym.*, **251**, 876 (1973).
22. J. Rathje and W. Ruland, *Colloid Polym. Sci.*, **254**, 358 (1976).
23. E. A. Porai-Koshits, *J. Non-Cryst. Solids*, **25**, 86 (1977).
24. H. Lee and K. Neville, *Epoxy Resins, Their Applications and Technology*, McGraw-Hill, New York, 1957.
25. T. P. Seward and D. R. Uhlmann, in *Amorphous Materials*, R. W. Douglas and B. Ellis, Eds., Wiley, New York, 1972.

Received August 27, 1979

Accepted November 6, 1979

## **On the Structure of Glassy Polymers. VI. Electron Microscopy of Polycarbonate, Poly(ethylene Terephthalate), Poly(vinyl Chloride), and Polystyrene**

M. MEYER,\* J. VANDER SANDE, and D. R. UHLMANN, *Department of Materials Science and Engineering, Center for Materials Science and Engineering, Massachusetts Institute of Technology, Cambridge, Massachusetts 02139*

### **Synopsis**

High-resolution electron microscopy studies have been carried out on four glassy polymers examined in previous small-angle x-ray scattering (SAXS) investigations. The polymers include polycarbonate, poly(ethylene terephthalate), poly(vinyl chloride), and polystyrene. For all four polymers, both bright-field and dark-field observations indicate the general absence of microstructural features of a size down to the resolution limit of the electron microscope. Only "pepper and salt" features on a scale ca. 5 Å are seen as characteristic of the structures. These features reflect simple interferences as the resolution limit is approached, and are seen for single crystals and oxide glasses as well as for the polymers. The present results, taken together with structural information from light scattering, SAXS, and small-angle neutron scattering, indicate that glassy polymers should be regarded as having random structures. The combined results are inconsistent with heterogeneous microstructures having regions of locally high order present in large volume fractions.

### **INTRODUCTION**

The past decade has seen much debate and many seemingly contradictory results on the structure of bulk amorphous polymers. There have been several structural models proposed in the literature, each providing an explanation for certain experimental results. Foremost among these are the random coil model, advanced forcefully by Flory and his associates<sup>1,2</sup> and the nodule model, advanced by Geil and Yeh and their associates.<sup>3,4</sup>

The random coil model pictures the unoriented amorphous bulk polymer as random in structure with isotropic properties. The configuration statistics of the molecule in bulk are expected to be the same as when dissolved in a  $\theta$  solvent. Rubber elastic behavior, light scattering, small-angle neutron scattering, magnetic birefringence, and small-angle x-ray scattering are among the experimental results which have provided support for this model.

The nodular bundle models assume that glassy polymers are inhomogeneous on a molecular level, with regions of disorder and regions of local order both present in large volume fractions. The principal experimental results which have provided support for this model are transmission electron microscope observations, although other results such as those obtained in x-ray diffraction studies have also been discussed in terms of regions of locally high order.

Because of their relevance to the present investigation, it seems appropriate

\* Based in part on a thesis submitted by M.M. in partial fulfillment of the requirements for the M.S. degree in Materials Science, Massachusetts Institute of Technology, 1978.

to review briefly the salient findings of the studies used to support the nodule hypothesis. Work dealing with four polymers—polycarbonate, polystyrene, poly(ethylene terephthalate), and poly(vinyl chloride)—will receive particular attention.

A precursor of the nodule model is discussed in the work of Krimm and Tobolsky,<sup>5</sup> who performed x-ray diffraction studies of polystyrene and poly(methyl methacrylate). For both polymers, diffraction peaks suggested to be associated with interchain distances were identified, and were indicated to change systematically with thermal treatment. It was suggested that small ordered regions were present in both polymers, with the size of the ordered regions being smaller in the case of poly(methyl methacrylate) because of the presence of the bulky side groups.

Bjornhaug et al.<sup>6</sup> expanded on the work of Krimm and Tobolsky by applying radial distribution analysis to the x-ray diffraction patterns. For polystyrene the peak intensities at 5 and 10 Å were suggested to be higher than expected for a random conformation, and were explained by postulating the existence of ordered regions in the amorphous polymers.

Yeh and Geil<sup>7</sup> used a solution-casting technique to prepare specimens of glassy poly(ethylene terephthalate) for transmission electron microscopy. They reported the presence of ball-like structures, 45–100 Å in size, as an essential structural feature of the material. These features were termed nodules. Subsequent observation, after annealing near the glass transition, showed the structures to have aggregated and aligned. Extensive annealing over a 6-day period at 66°C resulted in the formation of spherulites. At 154°C, the spherulites were formed in 15 min. Dark-field electron microscopy, carried out using a portion of the most intense diffuse halo of the electron diffraction pattern, indicated heterogeneities of about the same size as those seen under bright-field conditions.

Carr et al.<sup>8</sup> carried out electron microscope studies of polycarbonate and reported the presence in large volume fraction of nodular units about 125 Å in size. These structural features were reported to enlarge upon annealing at temperatures near the glass transition. The nodules were suggested to represent regions of locally high order.

Klement and Geil<sup>9</sup> carried out an electron microscope study of solution-cast specimens of isotactic polystyrene (i-PS), isotactic poly(methyl methacrylate) (i-PMMA), and polycarbonate (PC). After observing the as-cast structures, the polymers were drawn uniaxially at a controlled temperature: 105–125°C for PC, 55–70°C for PMMA, and 95–110° for PS.

The as-cast morphology of PC consisted of 100-Å nodules which grew and merged into a spherulitic structure upon annealing. The postdeformation morphology consisted of rows of thick and thin polymer aligned perpendicular to the drawn direction and spaced 1000 Å apart. It was suggested that the 100-Å nodules were composed of closely packed chains which were drawn out during deformation.

The as-cast i-PMMA was also amorphous by electron diffraction, but electron micrographs of samples shadowed with carbon–platinum revealed a 150–200-Å nodular structure. Samples which had been drawn to four times their original length exhibited 700–800-Å undulations. The nodules were suggested to be composed of closely packed chains, as in PC. The as-cast i-PS films were amorphous and structureless above 100 Å. Drawn films had surface undulations which resembled those of PMMA.

Yeh<sup>9</sup> investigated the nodular structures found in PS. Neither tacticity, molecular weight, nor the molecular weight distribution of the atactic polymer changed the electron diffraction pattern. The nodular features, interpreted as regions of local order, were about 15–45 Å in diameter in the freshly prepared samples. Upon irradiation for 60 sec in the electron microscope, the location of a diffraction ring initially at 4.78 Å—suggested as arising from orderly chain packing—was observed to change to larger *d* spacings; and evidence of increasing line broadening and decreasing intensity with increasing irradiation was also noted.

Nodular structures about 200 Å in diameter were seen<sup>11</sup> in ion-etched rigid poly(vinyl chloride) (PVC). No such structures were seen, however, in freeze-fractured samples of this polymer,<sup>12</sup> although similar features were observed in freeze-fractured samples of plasticized PVC.

The conclusions of these studies—that glassy polymers are composed of regions of disorder and regions of locally high order—have been called into serious doubt by a number of recent experimental studies. Among these, three groups of investigations seem deserving of particular note:

1) *Light scattering.* Patterson<sup>13</sup> investigated the effects of cooling on light scattering from PMMA and PC. No evidence was found for an increase in the number density or size of heterogeneities in the polymers as the temperature was lowered, as would be expected for nodular structures as regions of local order.

2) *Small-angle x-ray scattering.* The small-angle x-ray scattering from a variety of polymers, including PC, PMMA, PET, PVC, and PS, has been shown<sup>14</sup> to be inconsistent both in magnitude and in angular dependence with the presence of nodular structures as representative of the bulk material.

3) *Small-angle neutron scattering.* Among studies of small-angle neutron scattering from amorphous polymers, that of Benoit<sup>15</sup> can be taken as representative. The radii of gyration of eight molecular weight polystyrene polymers were found to be the same, within experimental error, as those of the polymers in a # solvent (where the random coil is widely acknowledged as providing a useful representation of the chain conformation).

Taken *in toto*, these findings cast strong doubts on the validity of the electron microscope observations which suggested the occurrence of nodular structures as essential features of amorphous polymers. It seemed highly desirable, therefore, to reexamine the structure of glassy polymers using the technique of high-resolution electron microscopy. The present paper reports the results of such a reexamination.

## EXPERIMENTAL PROCEDURE

The polymers studied in this investigation were bisphenol-A polycarbonate (PC), amorphous poly(ethylene terephthalate) (PET), poly(vinyl chloride) (PVC), and polystyrene (PS). The samples were obtained from the same stock as those used in previous small-angle x-ray scattering studies<sup>14,16–18</sup>; the characteristics of the materials are cited in the previous papers.

The specimens were prepared for transmission electron microscopy using variations of the procedures employed by Geil and his co-workers. In the case of PC, 1.1 g of PC was dissolved in 40 ml of cyclohexanone. A clean glass slide was dipped into the solution. The slide was removed, and the solution allowed

to evaporate. The slide was dipped into distilled water, the polymer film floated off, and a portion of the film was picked up on a copper grid.

In the case of PET, 1.05 g of PET was dissolved in 40 ml of phenol. A carbon-coated grid was dipped directly into the solution, and the solvent was allowed to evaporate. The sample used for the bright-field-dark-field pair was made then. The samples used in the through-focal series were made two days later. The solution was first centrifuged to remove a hazy suspension, and the clear liquid decanted off and used in making the sample.

In the case of PVC, 602 g of PVC was added to 30 ml of nitrobenzene to form a saturated solution. For PS, 1.4 g of PS was dissolved in 40 ml of methylethyl ketone. In each case the grid was dipped directly into the solution, and the solvent allowed to evaporate.

In those cases where a carbon film was used to support the polymer, the carbon substrate was about 150 Å thick and the polymer was always at least four times this thickness. In all cases, the grids with sample attached were coated with a thin carbon layer to minimize problems of sample instability in the electron beam.

The specimens were examined in a Siemens Elmiskop 101 electron microscope operating at 80 or 100 kV. This instrument is a modern, high-resolution electron microscope with a resolution of 3.5 Å point-to-point. The specimens were viewed in both bright field and dark field. The dark-field observations were accomplished using the second diffuse halo centered on the optics axis. An objective aperture of 25 μm was used. The sequence of images was usually the dark-field image (requiring an exposure time of about 30 sec) followed by a bright-field image of the same area (exposure time about 4 sec). It was determined that the reverse sequence (bright field preceding dark field) yielded identical results. In all cases, the micrographs were taken using the full resolution of the instrument (with magnifications of  $\times 500,000$  or more on the photographic plates). In some cases, through-focus series of micrographs were taken to explore the effect of focus condition on the apparent structure.

## RESULTS

### Polycarbonate

A representative bright-field electron micrograph of polycarbonate is shown to the left in Figure 1. It is seen that the material is structureless (featureless) down to the limit of resolution of the electron microscope. Only the "pepper and salt" structure characteristic of electron micrographs taken at high resolution is seen. The "pepper and salt" structure observed is a result of the use of a finite objective aperture to limit the amount of information (in the form of transmitted or scattered electrons) exiting the object that is used to construct the image. That is to say, the original object convoluted with the transform of the circular objective aperture (an Airy disk) yields the form of the image.<sup>19a</sup> If the object is considered to be an array of atoms or molecules, then the convolution of the object with an Airy disk (the aperture transform) will yield a blurred image of the array observed as the "pepper and salt" structure.

The corresponding dark-field image of the same area is shown to the right in Figure 1. Again, no evidence of any nodular features is seen; and the combination of the bright-field and dark-field micrographs provides strong evidence for a highly homogeneous structure.

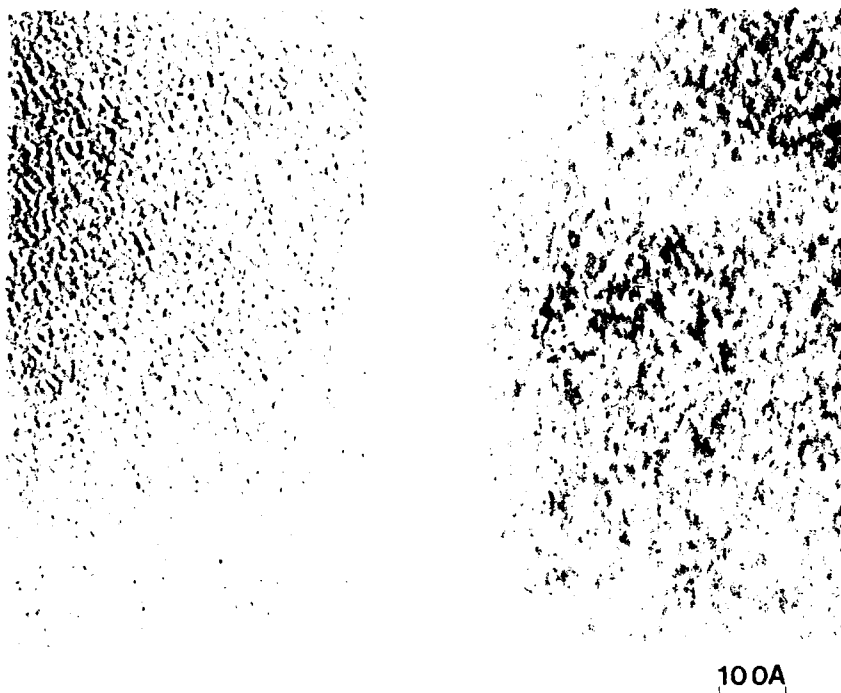


Fig. 1. Corresponding bright-field (left) and dark-field (right) electron micrographs of polycarbonate.

#### Poly(ethylene Terephthalate)

A representative bright-field electron micrograph is shown to the left in Figure 2; the corresponding dark-field micrograph of the same area is shown to the right in Figure 2. Again the material is seen to be featureless down to the limit of resolution of the electron microscope.

Since PET was the first polymer for which distinct nodular structures in the glassy state were reported, and since the nodules in this material appear with greater clarity than those in other polymers, it was decided to subject PET to even closer scrutiny. Several through-focus series of micrographs were taken, a representative set of which is shown in Figure 3. This series shows the absence of perceivable structure in the in-focus micrograph, and illustrates how apparent structure can be developed in the micrographs by going to either an underfocus or an overfocus condition. Using the arguments above, the change in the scale of the salt and pepper noted with change in focus can be considered as an additional defocus convolution with the original object.

#### Poly(vinyl Chloride) and Polystyrene

Representative bright-field and dark-field electron micrographs of the same area of the poly(vinyl chloride) sample and polystyrene sample are shown in Figures 4 and 5, respectively. It is seen that these polymers are also featureless down to the resolution of the electron microscope. No evidence is found for nodule-type heterogeneities; only the "pepper and salt" structure is noted.

For all four polymers, occasional discrete heterogeneities were seen. These heterogeneities are usually crystalline in nature, and are present in small volume fractions (typically less than 1%). The origin and characteristics of these heterogeneities was not examined in detail.

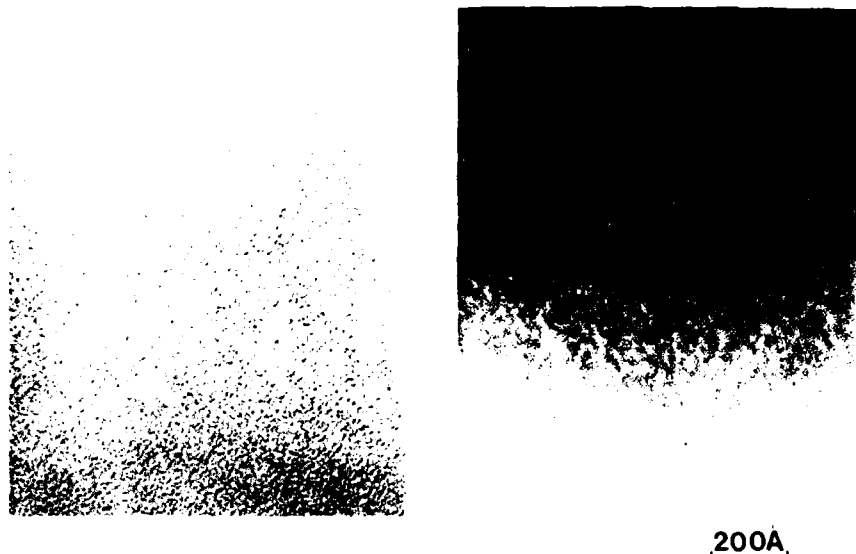


Fig. 2. Corresponding bright-field (left) and dark-field (right) electron micrographs of poly(ethylene terephthalate).

## DISCUSSION

The results of the present investigation of four glassy polymers, carried out using a modern high-resolution electron microscope, indicate the absence of any observable heterogeneities present in sizable volume fractions in any of the polymers. When viewed in either bright field or dark field, each of the polymers appears featureless down to the limit of resolution of the electron microscope. When viewed at very high magnifications, only the pepper and salt features on a scale ca. 5 Å are seen as characteristic of the polymer. Such pepper and salt features are seen in all materials, even single crystals and oxide glasses, when observations are carried out near the resolution limit of the electron microscope.

These results indicate that the microstructure of all four polymers - PC, PET, PVC, and PS - is featureless down to a scale below 10 Å. Similar featureless microstructures have previously been observed for single-component oxide glasses such as fused silica<sup>19</sup>; it is suggested that these glassy polymers, like the oxide glasses, should be regarded as random arrays in which no unit of structure is repeated at regular intervals in three dimensions.

The through-focus series of electron micrographs, an example of which is shown in Figure 3, indicate the absence of structural features when in focus and the development of such features when out of focus. That is, the samples are featureless down to about the resolution limit of the electron microscope when in focus; but out-of-focus conditions can lead to the pepper and salt being seen as apparent structure on a scale notably greater than the resolution limit. When taking micrographs at high magnifications, particularly under dark-field conditions, it is difficult to achieve exact focus conditions, and correspondingly easy to observe apparent structure on a fine scale as a result of instrumental artifacts.

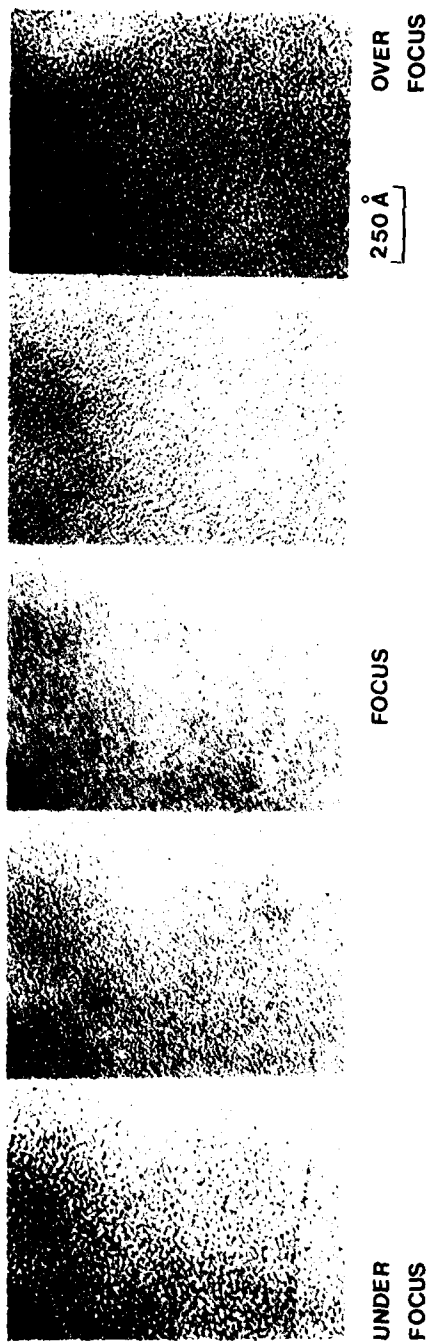


Fig. 3. Through-focus series of electron micrographs of poly(ethylene terephthalate) showing the absence of structural features when in focus and the development of apparent structural features when out of focus.

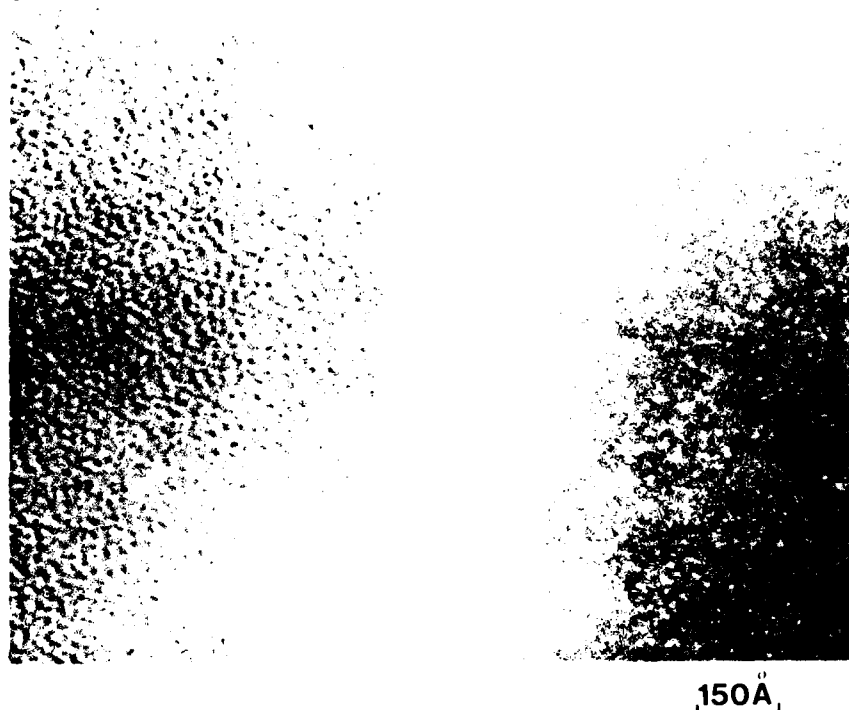


Fig. 4. Corresponding bright field (left) and dark field (right) electron micrographs of poly(vinyl chloride).

The results of the present electron microscope study are therefore in accord with the findings of other investigations of glassy polymers, such as the light scattering, small-angle x-ray scattering and small-angle neutron scattering work discussed in the Introduction. It remains only to consider the wide-angle x-ray diffraction studies which have been taken as providing direct structural evidence for regions of local order in glassy polymers.

In assessing the results of the x-ray diffraction studies, it should first be noted that the ability to obtain critical insight into the structure of amorphous materials depends on the reliability of the scattering data at intermediate-to-large values of  $\sin \theta/\lambda$ . Here  $\theta$  is the scattering angle and  $\lambda$  is the wavelength of the radiation used. Unfortunately, for materials composed of elements of small atomic number such as polymers, the Compton modified intensity which contains no structural information often comprises the bulk (perhaps as much as 90%) of the measured intensity at large values of  $\sin (\theta/\lambda)$ . This large modified scattering must be separated from the coherently diffracted intensity by a theoretical correction which introduces considerable uncertainty into the precise form of the data.

A second problem is introduced by the use of the "proportionality of scattering factors" approximation, which is used to effect a Fourier inversion and obtain the radial distribution function from diffraction data. The approximation assumes that the  $\sin (\theta/\lambda)$  dependence of the scattering factors for all atoms in the glass is the same. Unfortunately, this is a poor assumption for many glassy polymers (e.g., PC), and introduces an error of unspecified form in the results.

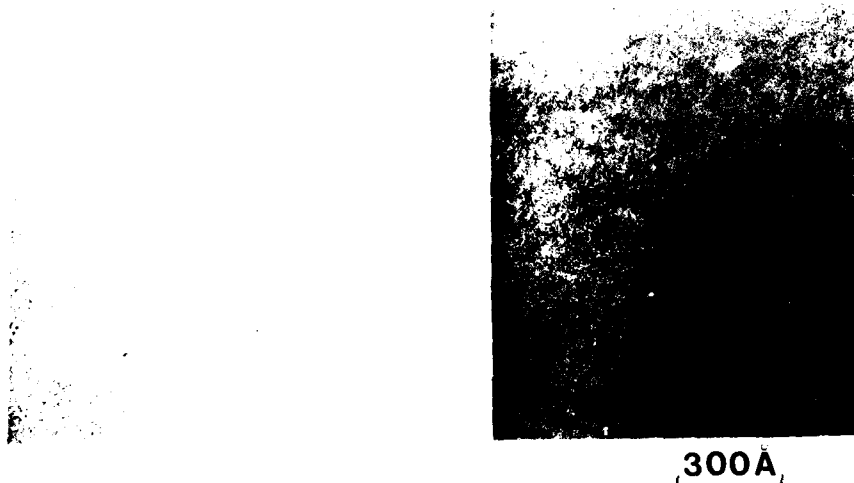


Fig. 5. Corresponding bright-field (left) and dark-field (right) electron micrographs of polystyrene.

The studies cited above as providing evidence for local order in glassy polymers encountered both of these problems; and these problems limit substantially the confidence which can be placed in the conclusions. More recent x-ray diffraction studies of glassy polymers<sup>20</sup> have suggested that little intermolecular ordering occurs. The recent studies have generally employed improved experimental techniques, but still have analyzed the data in terms of radial distribution functions (and hence still have used the proportionality of scattering factors approximation).

The large Compton scattering component at high  $\sin(\theta/\lambda)$  can experimentally be reduced or eliminated by the use of double-crystal monochromators or fluorescence detectors; the proportionality of scattering factors approximation can be eliminated by avoiding the Fourier inversion and describing the structure in terms of pair correlation functions. These techniques are discussed at length in ref. 21. To date, such techniques do not appear to have been applied in published studies of amorphous polymers, however, a recently completed investigation of polycarbonate which does utilize these techniques<sup>22</sup> indicates that the frequently occurring distances in this polymer can be described as intrachain distances.

The results of the present electron microscope study are then in accord with wide-angle x-ray diffraction data as well as the results of the other studies discussed above. The present findings are, however, at variance with those of the electron microscope studies discussed in the Introduction. Through-focus series of micrographs such as that shown for PET in Figure 3 suggest that the fine-scale (<20 Å) apparent structure seen in some previous investigations may simply reflect the use of electron microscopes of insufficient resolution, or may result from the lack of proper focus in taking the micrographs. Neither of these possibilities can be confirmed at present, nor can alternative explanations based on other effects such as radiation damage from the electron beam or the possibility that the observed nodules represent surface features of the polymers.

It seems clear from the present work that the nodular structures should not be taken as representative of the microstructures seen in electron microscope examination of glassy polymers. It also seems clear that random array models, such as the random coil model, are generally in accord with the electron microscope results as well as with the results of a variety of other structural investigations and determinations of properties.

### CONCLUSIONS

The microstructures of four glassy polymers—polycarbonate, poly(ethylene terephthalate), poly(vinyl chloride), and polystyrene—have been examined using high-resolution electron microscopy. In all cases, the microstructures are generally featureless down to the limit of resolution of the electron microscope. Only the pepper and salt features characteristic of microscope operation near the resolution limit are seen. Both bright-field and dark-field electron microscopy indicate featureless microstructures, with occasional evidence for discrete heterogeneities present in very small volume fractions.

The present results are in accord with data obtained from light scattering, small-angle x-ray scattering, and small-angle neutron scattering in suggesting that the structures of glassy polymers be represented as random arrays. The results are at variance with observations of previous electron microscope studies which indicated the presence of nodular features. It has been shown here that features like the fine-scale nodules can be produced by out-of-focus conditions on electron micrographs, conditions which often obtain in taking micrographs at high magnifications.

Financial support for the present work was provided by the Air Force Office of Scientific Research. This support is gratefully acknowledged.

Aerospace Research Laboratories  
AFOSR-77-3226

### References

1. P. J. Flory, *J. Macromol. Sci. Phys.*, **B12**, 1 (1976).
2. D. Y. Yoon and P. J. Flory, *Polymer*, **16**, 645 (1975).
3. P. H. Geil, *Morphology of Amorphous Polymers*, Final Report USAROD, Contract DAHC04-70C-0032.
4. G. S. Y. Yeh, *Crit. Rev. Macromol. Chem.*, **1**, 173 (1972).
5. S. Krimm and A. V. Tabolsky, *Textile Res. J.*, **21**, 805 (1951).
6. A. Bjornhaug, O. Ellefsen, and B. A. Tonnesen, *J. Polym. Sci.*, **12**, 621 (1954).
7. G. S. Y. Yeh and P. H. Geil, *J. Macromol. Sci. Phys.*, **B1**, 235 (1967).
8. S. H. Carr, P. H. Geil, and E. Baer, *J. Macromol. Sci. Phys.*, **B2**, 13 (1968).
9. J. J. Klement and P. H. Geil, *J. Macromol. Sci. Phys.*, **B6**, 31 (1972).
10. G. S. Y. Yeh, *J. Macromol. Sci. Phys.*, **B6**, 451 (1972).
11. P. M. Gezovich and P. H. Geil, *Int. J. Polym. Mater.*, **1**, 3 (1971).
12. C. Singleton, J. Isner, D. M. Gezovich, P. K. C. Tsou, P. H. Geil, and E. A. Collins, *Polym. Eng. Sci.*, **14**, 371 (1974).
13. G. Patterson, *J. Macromol. Sci. Phys.*, **B12**, 61 (1976).
14. A. L. Renninger, G. G. Wicks, and D. R. Uhlmann, *J. Polym. Sci.*, **13**, 1247 (1975).
15. H. Benoit, *J. Macromol. Sci. Phys.*, **B12**, 27 (1976).
16. A. L. Renninger and D. R. Uhlmann, *J. Polym. Sci.*, **14**, 415 (1976).
17. R. S. Straff and D. R. Uhlmann, *J. Polym. Sci.*, **14**, 353 (1976).
18. A. L. Renninger and D. R. Uhlmann, *J. Polym. Sci.*, to be published.
19. T. P. Seward and D. R. Uhlmann, *Amorphous Materials*, R. W. Douglas and B. Ellis, Eds., Wiley, New York, 1972, pp. 327–336.
- 19a. C. A. Taylor and H. Lipson, *Optical Transforms*, Cornell U. P., New York, 1964.
20. G. D. Wignall and G. W. Longman, *J. Mater. Sci.*, **8**, 1439 (1973).
21. B. E. Warren and R. L. Mozzi, *J. Appl. Crystallogr.*, **3**, 59 (1970).
22. G. G. Wicks and D. R. Uhlmann, *J. Polym. Sci.*, to appear.

Received February 27, 1978.

Revised May 16, 1978.